

WOLF CREEK

NUCLEAR OPERATING CORPORATION

Stephen E. Hedges
Vice President Operations and Plant Manager

May 3, 2007
WO 07-0012

U. S. Nuclear Regulatory Commission
ATTN: Document Control Desk
Washington, DC 20555

- Reference:
- 1) Letter ET 06-0004, dated February 21, 2006, from T. J. Garrett, WCNOG, to USNRC
 - 2) Letter dated June 27, 2006, from J. N. Donohew, USNRC, to R. A. Muench, WCNOG
- Subject: Docket No. 50-482: Response to Request for Additional Information Related to License Amendment Request to Revise the Steam Generator Program

Gentlemen:

Reference 1 provided Wolf Creek Nuclear Operating Corporation's (WCNOG) application to revise Technical Specification 5.5.9, "Steam Generator Tube Surveillance Program," to exclude portions of the tube below the top of the tubesheet in the Wolf Creek Generating Station (WCGS) steam generators from periodic steam generator tube inspections. Amendment No. 164 dated May 8, 2006, revised the title of TS 5.5.9 to "Steam Generator (SG) Program." Reference 2 provided a request for additional information (RAI) based on the NRC staff review of Reference 1.

Attachment I provides responses to questions 23 and 24. Attachment II provides revised markups of changes to the current TSs. Enclosure I provides responses to questions 1-22 and questions 25 and 26. Enclosure IV provides Westinghouse Electric Company LLC LTR-CDME-07-91, "Replacement Figures to Update the Wolf Creek Technical Justification of H*/B*."

Enclosure I provides the proprietary Westinghouse Electric Company LLC LTR-CDME-07-72-P, "Response to NRC Request for Additional Information on Wolf Creek Generating Station (WCGS) Permanent B* License Amendment Request." Enclosure II provides the non-proprietary Westinghouse Electric Company LLC LTR-CDME-07-72-NP, "Response to NRC Request for Additional Information on Wolf Creek Generating Station (WCGS) Permanent B* License Amendment Request." Enclosure IV provides the proprietary Westinghouse Electric Company LLC LTR-CDME-07-91-P, "Replacement Figures to Update the Wolf Creek Technical Justification of H*/B*." As Enclosure I contains information proprietary to Westinghouse Electric Company LLC, it is supported by an affidavit signed by Westinghouse Electric Company LLC, the owner of the information. The affidavit sets forth the basis on which the information may be withheld from public disclosure by the Commission and addresses with specificity the considerations listed in paragraph (b)(4) of 10 CFR 2.390 of the Commission's regulations. Accordingly, it is respectfully requested that the information, which is proprietary to Westinghouse, be withheld from public disclosure in accordance with 2.390 of the Commission's regulations. This affidavit, along with Westinghouse authorization letter, CAW-07-2273, "Application for Withholding Proprietary Information from Public Disclosure," is contained in Enclosure III.

The additional information provided in the Attachments and Enclosures do not impact the conclusions of the No Significant Hazards Consideration provided in Reference 1. In accordance with 10 CFR 50.91, a copy of this submittal is being provided to the designated Kansas State official.

This letter contains no commitments. If you have any questions concerning this matter, please contact me at (620) 364-4190, or Mr. Kevin Moles at (620) 364-4126.

Very truly yours,



Stephen E. Hedges

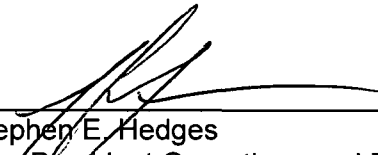
SEH/rt

Attachments
Enclosures

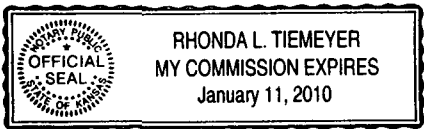
cc: T. A. Conley (KDHE), w/a, w/e
J. N. Donohew (NRC), w/a, w/e
V. G. Gaddy (NRC), w/a, w/e
B. S. Mallett (NRC), w/a, w/e
Senior Resident Inspector (NRC), w/a, w/e

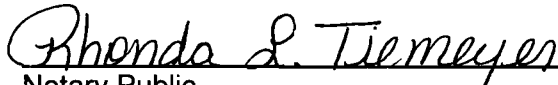
STATE OF KANSAS)
) SS
COUNTY OF COFFEY)

Stephen E. Hedges, of lawful age, being first duly sworn upon oath says that he is Vice President Operations and Plant Manager of Wolf Creek Nuclear Operating Corporation; that he has read the foregoing document and knows the contents thereof; that he has executed the same for and on behalf of said Corporation with full power and authority to do so; and that the facts therein stated are true and correct to the best of his knowledge, information and belief.

By 
Stephen E. Hedges
Vice President Operations and Plant Manager

SUBSCRIBED and sworn to before me this 3rd day of May, 2007.




Notary Public

Expiration Date January 11, 2010

RESPONSE TO REQUEST FOR ADDITIONAL INFORMATION

The Nuclear Regulatory Commission (NRC) request for additional information (RAI) dated June 27, 2006. The RAI is based on the NRC staff review of the WCNOG license amendment request dated February 21, 2006 (letter ET 06-0004). This Attachment provides Wolf Creek Nuclear Operating Corporation (WCNOG) specific responses to questions 23 and 24. Enclosure I provides responses to questions 1-22 and questions 25 and 26.

23. *By letter dated March 28, 2006 (ADAMS Accession No. ML060940425), the licensee provided revisions to the proposed TSs in accordance with Technical Specification Task Force (TSTF)-449, Revision 4, to include the following additional sentence into TS 5.5.9 c.1: "All tubes with degradation identified in the portion of the tube within the region from the top of the hot leg tubesheet to 17 inches below the top of the tubesheet shall be removed from service." Describe the plans for revising these words to reflect the February 21, 2006, license amendment and for submitting revisions to this amendment.*

RESPONSE: At the time of submittal of letter ET 06-0004, the NRC had not approved the revisions proposed to TS 5.5.9 that incorporated Technical Specification Task Force (TSTF)-449, Revision 4. In Attachment III to ET 06-0004, WCNOG provided proposed changes to TS 5.5.9 based on incorporation of change associated with TSTF-449, Revision 4. Specifically, c.1 was revised as follows:

"For tubes fully expanded into the tubesheet, degradation found in the portion of the tube below the depth identified in the below tables from the top of the tubesheet does not require plugging."

No additional revisions to the license amendment request or to the TSs are necessary.

24. *Discuss the plans to revise TS 5.6.10 to include reporting requirements applicable to the implementation of the tubesheet inspection and alternate repair criteria. For example:*
- *A breakout of indications detected within the tubesheet inspection depths with respect to their location, orientation, and measured size. (The only difference here relative to proposed changes associated with TSTF-449, Rev. 4, is that the indications in the tubesheet region would be listed separately from those elsewhere.)*
 - *The operational primary-to-secondary leakage rate observed in each SG during the cycle preceding the inspection, which is the subject of the report, and the calculated accident leakage rate for each steam generator from the portion of tubing below the tubesheet inspection depths for the most limiting accident. If the calculated accident leakage rate for any SG is less than 2 times the total observed operational primary-to-secondary leakage rate, the 12-month report should describe how it was determined.*

RESPONSE: WCNOG is proposing to revise TS 5.6.10, "Steam Generator Tube Inspection Report," to include three additional reporting requirements. The additional items address the

reporting details regarding indications detected in the portion of the tube above the depths identified in the TS tables in TS 5.5.9 c.1., the primary to secondary LEAKAGE rate observed in the previous operating cycle, and the calculated accident leakage rate from the portion of the tubes below the depths identified in the TS tables in TS 5.5.9 c.1.

Attachment II provides the proposed changes to TS 5.6.10.

Changes to TS 5.5.9c.1

Letter ET 06-0004 proposed changes to TS 5.5.9c.1, indicating that for tubes fully expanded into the tubesheet, degradation found in the portion of the tube below the depth identified in specified tables from the top of the tubesheet do not require plugging. The resolution of request for additional information resulted in the recalculation of the safety significant portion of the tube within the tubesheet. Enclosure IV provides Westinghouse Electric Company LLC LTR-CDME-07-91-P, "Replacement Figures to Update the Wolf Creek Technical Justification of H*/B*," which is the result of the recalculation. Enclosure IV provides revised Figures 11-3 and 11-4 and Table 11-2 from LTR-CDME-05-0209-P, ""Steam Generator Tube Alternate Repair Criteria for the Portion of the Tube Within the Tubesheet at the Wolf Creek Generating Station." Enclosure I to ET 06-0004 provided LTR-CDME-05-0209-P. Attachment II provides proposed changes to TS 5.5.9c.1 based on Enclosure IV.

Revised Markups of Current Technical Specification Pages

5.5 Programs and Manuals

5.5.9 Steam Generator (SG) Program (continued)

3. The operational LEAKAGE performance criterion is specified in LCO 3.4.13, "RCS Operational LEAKAGE."

c. Provisions for SG tube repair criteria. Tubes found by inservice inspection to contain flaws with a depth equal to or exceeding 40% of the nominal tube wall thickness shall be plugged.

The following alternate tube repair criteria may be applied as an alternative to the 40% depth-based criteria:

the depth identified in the below tables

1. For Refueling Outage 15 and the subsequent operating cycle, degradation found in the portion of the tube below 17 inches from the top of the hot leg tubesheet does not require plugging. All tubes with degradation identified in the portion of tube within the region from the top of the hot leg tubesheet to 17 inches below the top of the tubesheet shall be removed from service.

INSERT 5.D-12

d. Provisions for SG tube inspections. Periodic SG tube inspections shall be performed. The number and portions of the tubes inspected and methods of inspection shall be performed with the objective of detecting flaws of any type (e.g., volumetric flaws, axial and circumferential cracks) that may be present along the length of the tube, from the tube-to-tubesheet weld at the tube inlet to the tube-to-tubesheet weld at the tube outlet, and that may satisfy the applicable tube repair criteria. For Refueling Outage 15 and the subsequent operating cycle, the portion of the tube below 17 inches from the top of the hot leg tubesheet is excluded. The tube-to-tubesheet weld is not part of the tube. In addition to meeting the requirements of d.1, d.2, and d.3 below, the inspection scope, inspection methods, and inspection intervals shall be such as to ensure that SG tube integrity is maintained until the next SG inspection. An assessment of degradation shall be performed to determine the type and location of flaws to which the tubes may be susceptible and, based on this assessment, to determine which inspection methods need to be employed and at what locations.

identified in c.1 above

1. Inspect 100% of the tubes in each SG during the first refueling outage following SG replacement.

For tubes fully expanded into the tubesheet,

(continued)

INSERT 5.0-12

STEAM GENERATOR TUBE INSPECTION DEPTHS

STEAM GENERATOR HOT LEG				
Inspection Depth Zones	H1	H2	H3	H4
Radius of the Zone from the Vertical Centerline of the Tubesheet (inches)	2 - 28	>28 - 36	>36 - 48	>48 - 59
Depth for the Zone (inches)	11.0	9.0	7.0	4.0

STEAM GENERATOR COLD LEG				
Inspection Depth Zones	C1	C2	C3	C4
Radius of the Zone from the Vertical Centerline of the Tubesheet (inches)	2 - 26	>26 - 38	>38 - 50	>50 - 59
Depth for the Zone (inches)	12.0	10.5	8.0	5.0

5.6 Reporting Requirements

5.6.10 Steam Generator Tube Inspection Report

A report shall be submitted within 180 days after the initial entry into MODE 4 following completion of an inspection performed in accordance with the Specification 5.5.9, Steam Generator (SG) Program. The report shall include:

- a. The scope of inspections performed on each SG;
- b. Active degradation mechanisms found;
- c. Nondestructive examination techniques utilized for each degradation mechanism;
- d. Location, orientation (if linear), and measured sizes (if available) of service induced indications;
- e. Number of tubes plugged during the inspection outage for each active degradation mechanism;
- f. Total number and percentage of tubes plugged to date; and
- g. The results of condition monitoring, including the results of tube pulls and in-situ testing.

INSERT 5.0-26 →

INSERT 5.0-26

- h. The number of indications and location, size, orientation, and whether initiated on primary or secondary side for each indication detected in the portion of the tube above the depths identified in the Tables in TS 5.5.9 c.1.;
- i. The primary to secondary LEAKAGE rate observed in each SG (if it is not practical to assign the LEAKAGE to an individual SG, the entire primary to secondary LEAKAGE should be conservatively assumed to be from one SG) during the cycle proceeding the inspection which is the subject of the report; and
- j. The calculated accident leakage rate from the portion of the tubes below the depths identified in the Tables in TS 5.5.9 c.1. for the most limiting accident in the most limiting SG. In addition, if the calculated accident leakage rate from the most limiting accident is less than 2 times the maximum primary to secondary LEAKAGE rate, the report should describe how it is determined.

Enclosure II to WO 07-0012

**Westinghouse Electric Company LLC LTR-CDME-07-72-NP "Response to NRC Request
for Additional Information on the Wolf Creek Generating Station (WCGS) Permanent
B* License Amendment Request"
(NON-PROPRIETARY)**

LTR-CDME-07-72 NP-Attachment

Wolf Creek Nuclear Operating Corporation

**Response to NRC Request for Additional Information Relating to LTR-CDME-05-209-P of the Wolf
Creek Generating Station (WCGS) Permanent B* License Amendment Request**

April 24, 2007

Westinghouse Electric Company LLC
P.O. Box 158
Madison, PA 15663
©2007 Westinghouse Electric Company LLC
All Rights Reserved

Wolf Creek Generating Station (WCGS) Permanent B* Responses to NRC Request for Additional Information

Steam Generator Tube Alternate Repair Criteria
for the Portion of the Tube Within the Tubesheet
at the Wolf Creek Generating Station
(LTR-CDME-05-209-P)

Wolf Creek Nuclear Operating Corporation (WCNOC) submitted a license amendment request on February 21, 2005 (letter ET 06-0004), proposing changes to the Technical Specifications for WCGS. The proposed changes are to revise Technical Specification 5.5.9, "Steam Generator Tube Surveillance Program," to exclude portions of the steam generator tube below the top of the tubesheet in the steam generators from periodic tube inspections based on the application of structural analysis and leak rate evaluation results to re-define the primary-to-secondary pressure boundary. The NRC staff provided a Request for Additional Information (RAI) on June 27, 2006. Throughout the response, reference is made to LTR-CDME-05-0209-P. Enclosure 1 to WCNOC letter ET 06-0004 provided LTR-CDME-05-0209-P which is the technical justification of H*/B* for Wolf Creek.

It is important to note that since the NRC RAI was received in June of 2006, other licensees have submitted similar requests for TS changes, although not at the same inspection depth, in response to which the NRC issued requests for additional information. Westinghouse believes that the development of responses for the other licensees has in some instances obviated some of the specific RAIs provided to Wolf Creek. Further, additional test data became available in November 2006 that altered a fundamental assumption in the analysis provided in LTR-CDME-05-0209-P. The impact of the new test data, together with an improved structural analysis to address potential divider plate degradation issues was summarized in a "White Paper" which is included in these responses as Appendix A. The responses developed below to the RAI provided to Wolf Creek by the NRC incorporate all new information developed through related licensing actions by other utilities since June 2006.

Provided below are responses to the RAIs.

- 1. Enclosure 1 of the application, Sections 6.1 and 6.2 - What were the actual yield strengths and wall thicknesses of the tube specimens used for pullout and leakage testing? How do these values compare to minimum values of these parameters at Wolf Creek? Discuss the effect of tube yield strength and wall thickness on contact pressure between the tube and tubesheet after the tube expansion process (i.e., ignoring pressure and temperature loads). Discuss why the test specimen strengths and wall thicknesses were conservative from the standpoint of minimizing the contact pressures between the tube and tubesheet, or discuss what adjustments need to be made to test results to allow for the variability of yield strength and tube wall thickness.*
- 2. Enclosure 1, Section 6.2.1 - The section states that the leak test program utilized tubesheet simulants (collars) with the nominal tubesheet hole diameter. Was this also the case for the pullout tests? What were the diameters of the tube specimens used in the pullout and leakage tests? Discuss the effect that the field tolerances on these parameters can have on contact*

pressure between the tube and tubesheet after the tube expansion process (i.e., ignoring pressure and temperature loads). Discuss why the parameter values used for the test specimens were conservative from the standpoint of minimizing the contact pressures between the tube and tubesheet, or discuss what adjustments need to be made to test results to allow for the variability of these parameters.

Response to RAI 1 and 2

The hydraulic expansion process is shown schematically in Figure 1. The Wolf Creek tubes were first tack expanded to a depth of about 3/4 inch by a mechanical rolling process to facilitate welding of the tube to the cladding on the primary face of the tubesheet. (Later in time, the tack expansion process was changed to a urethane plug expansion process.) Following welding, the tube was hydraulically expanded through the full thickness of the tubesheet. A quick disconnect expansion gun connects to the end of the mandrel and supplies deionized water which passes through a hole down the axis of the mandrel and exits into the cavity between the tube and the mandrel. Pressurization of the water expands the tube. The pressure is held by the O-rings which are in turn squeezed against fixed metal rings. After the expansion, which takes only a few seconds, the water is withdrawn into the supply tank, the seals relax, and the mandrel is easily removed.

A generic description of the hydraulic expansion process follows: In the steam generators, the tubesheet is 21.03 inches thick and is made of low alloy steel, SA-508 Class 2. The tubing material is thermally treated Alloy 600 and is nominally 1 1/16 inch OD with a wall thickness of 0.040 inch. The radial gap (clearance between the unexpanded tube and the tubesheet hole) is []^{a,c,e}. Though it takes less than []^{a,c,e} pressure to expand the tube into contact with the tubesheet, the pressure is increased into a range of []^{a,c,e} depending on the tubing dimensions and properties. The depth of expansion – or equivalently, the secondary side crevice depth is controlled by the location of the urethane-metal ring interface relative to the secondary face of the tubesheet. The crevice depth is less than []^{a,c,e}.

The hydraulic expansion process is amenable to analytical modeling: The tube is uniformly expanded over the entire length of the tubesheet with monotonically increasing pressure. There is no redundant work of deformation. Soler and Hong, Weinstock, Reinis and Soler, and Singh and Soler have developed a theoretical incremental analysis which is very efficient for assessing the sensitivity of residual contact pressure to variations in tube and tubesheet geometry and material property parameters. This is a [

] ^{a,c,e} (Reference 1).

The reference modeling parameters used in the development of Figure 2 are:

a,c,e



- From Figure 2, the following can be concluded when a constant parameter variation within about $\pm 10\%$ is considered:
- The expansion pressure has the most significant influence on contact pressure which varies directly with expansion pressure. A 5% increase in expansion pressure yields a 33% increase in contact pressure.
- The yield strength of the tube has the second-most significant effect on contact pressure. The contact pressure varies inversely with yield strength. A 10% decrease in tube yield strength results in about a 45% increase in the contact pressure.
- Tube to tubesheet radial clearance is the third-most significant parameter that affects contact pressure in an inverse relationship. A 10% increase in clearance results in a little less than a 10% decrease in contact pressure.
- Less significant parameter variables are the elastic moduli (E) of the tube and of the tubesheet material. Within the limits of variability (approximately 2%) of these parameters, about an 8% decrease in contact pressure results when the tubesheet E is at its upper limit, and about a 5% increase in contact pressure results when the tube E is at its upper limit.

The hydraulic expansion process applicable to the manufacturing of the Wolf Creek steam generators specified an intensifier pressure control specification of []^{a,c,e}. This translates into an expansion pressure range of []^{a,c,e}. The mean yield strength for Alloy 600 thermally treated tubing utilized in the SGs reported in WCAP-12522 is []^{a,c,e}. The relationship between tube expansion pressure and residual joint contact pressure is provided in Figure 3. The effect of tube yield strength on interface pressure is shown in Figure 4. Assuming a tube yield strength of 50ksi, the predicted residual contact pressure of the hydraulically expanded joint is approximately []^{a,c,e}.

The test specimens for the pullout tests utilized an expansion pressure of 31,000 psi, Table 1 (see also RAI 4). The 0.2% offset yield strength for the tubing used in the pullout and leak rate testing was []^{a,c,e} which is conservatively high.

The effect of radial clearance on interface pressure (contact pressure) is shown in Figure 5. At the lower hydraulic expansion pressure of []^{a,c,e} the impact on residual contact pressure is minimal. The radial clearance is a function of both tubing outside diameter and tubesheet hole diameter.

Variation in tubesheet hole diameter was included in the tube pullout test results as the collar ID of the test specimens varied from []^{a,c,e}. The variation of tube outside diameter was less than 0.0003 inch. The known dimensions of the test specimens from the tests as reported in LTR-CDME-05-209-P are listed in Table 1 below. Westinghouse drawing number 1104J14 for the Wolf Creek SGs indicates a nominal tubesheet hole diameter of [] and a maximum of []^{a,c,e}. Therefore, since the pullout test specimen minimum collar hole dimensions varied from approximately the nominal tubesheet hole diameter to greater than the maximum SG tubesheet hole diameter, the tests provided conservatively low joint contact pressures in comparison to the contact pressures expected in the SGs.

In summary:

- The pullout tests specimens were made using an expansion pressure less than the mean expansion pressure of the SG manufacturing process specification. Therefore, in aggregate, the resulting test specimen contact pressures are conservatively low.
- The yield strength of the tubing used in the pullout test specimens was higher than the documented mean yield strength of prototypical SG tubing material. Therefore, the resulting test specimen contact pressures are conservatively low.
- The test specimen collar hole diameters exceeded the mean tubesheet hole diameters and included specimens that also exceeded the maximum tubesheet hole diameter. The tubing diameter is tightly controlled in the SGs and similarly, the tube diameter was practically invariant in the pullout tests. Therefore, the resulting test specimen contact pressures are conservatively low.
- The effect of tube wall thickness was shown to have negligible effect on tube joint contact pressure.

Based on the above, no further adjustments need to be made to the test results to allow for variability of yield strength and tube wall thickness.

As noted in LTR-CDME-05-209-P, a finite element model was developed for the Model F tubesheet, channel heads, and shell region to determine tubesheet hole dilations in the WCGS Unit 1 steam generators. A maximum tubesheet hole diameter of []^{a,c,e} was factored into the analysis.

Loads are imposed on the tube OD as a result of tube rotations under pressure and temperature conditions. The hole expansion calculation uses the FEA results and includes the effects of tubesheet rotations and deformations caused by the system pressures and temperatures. It does not include the local effects produced by interactions between the tubesheet and the tube. The effect of dimensional tolerances (tubesheet hole size) on the H*/B* analysis results can be accounted for in the local effects produced by the interactions between the tube and the tubesheet. The impact of a larger tubesheet hole diameter than in currently considered in the WCGS H* analysis is addressed below. A maximum outside radius of []^{a,c,e} has been considered in the local effects and the resultant impact on the values for H*/B* distances are included in Figure 6. This radius corresponds to a maximum tubesheet hole diameter of []^{a,c,e} (per drawing number 1104J14). Figure 6 also considers the new crevice pressure results as well as a divider plate factor of 1.00. The radius of the inner diameter of the tube is based on wall thinning in the tube equal to the average of that measured during hydraulic expansion tests as reported in LTR-CDME-05-209-P.

Figure 6 indicates that any variation in tube hole diameter from the nominal diameter used in the analysis will result in a []^{a,c,e}. For the WCGS Unit 1 steam generators of []^{a,c,e} in diameter, the impact on the existing H* distance at the worst case location is determined to be approximately []^{a,c,e}.



Figure 1: Schematic of the Hydraulic Expansion Mandrel

a,c,e



Figure 2: Model F Tube/Tubesheet Contact Pressure Sensitivity

a,c,e



Figure 3: Tube/Tubesheet Interface Pressure vs. Expansion Pressure

a,c,e



Figure 4: Tube/Tubesheet Interface Pressure vs. Tube Yield Strength

a,c,e



Figure 5: Tube/Tubesheet Interface Pressure vs. Radial Clearance



Figure 6: Plot of Maximum H* Depth as a Function of Tubesheet Hole Diameter for WCSG Unit 1

3. *Enclosure 1, Section 6.1, page 27 of 127 - Why was the pullout data evaluated at the lower 95th percentile? Discuss how this supports the ability of tubes to sustain pullout loads, versus using an absolute lower bound value? Given the limited number of tests performed (and the many thousands of tubes in the SGs), should not the lower bound value be evaluated to a high confidence value?*

Response

A flaw that is measured at the condition monitoring structural limit or the operational assessment repair limit must have a probability of 95% at a confidence level of 50% of satisfying the structural requirements is the acceptance standard used in EPRI Report TR-107621, "Steam Generator Integrity Assessment Guidelines: Revision 2." Evaluation of the pullout data at the lower 95th percentile is consistent with the existing standard. There are many other conservatisms that are contained in the test data and the analysis. For example, the performance requirement is to avoid burst at $3 \cdot \Delta P_{NOp}$ and $1.4 \Delta P_{SLB}$; therefore, the maximum pullout load could reasonably be considered or the load at the displacement where contact with an adjacent tube occurs could also reasonably be used. The use of the forces at the 0.25 inch displacement condition provides a conservative lower bound on the maximum to these values; therefore, the use of the probability of 95% at a confidence level of 50% value is a reasonable and conservative evaluation for the entire tube complement in a tube bundle.

4. Enclosure 1, Section 6.2.1.2 - The section states that the hydraulic expansion pressure was approximately [proprietary information]. Was hydraulic expansion pressure a measured parameter during SG fabrication that was used for acceptance of each joint? Was the lower limit of the acceptance standard the same as the lower limit of the assumed [proprietary information]? If the answer to either of these questions is no, what is the basis for the assumed [proprietary information]?

Response

The tube pullout test data presented in LTR-CDME-05-209-P is partially based on testing conducted for another Model F plant in 1997 where the expansion pressure range was between []^{a,c,e}. As a result, the majority of the expansion pressure test samples were expanded using a specified pressure of []^{a,c,e}. The remainder of the tube pullout test data presented in LTR-CDME-05-209-P is based on testing conducted in 1988 where the expansion pressure for the testing was []^{a,c,e}.

The WCGS steam generators were shipped in November of 1979. For steam generators built between early 1979 and 1981, the process specification revisions, (Rev. 4 through 10) only provide an intensifier pressure control specification of []^{a,c,e}. This translates into an expansion pressure range of []^{a,c,e}. Although the process was controlled and verified, the expansion pressure was not recorded for each tube during steam generator manufacture. Tubes that exceeded the maximum expansion pressure were addressed through deviation notices; tubes that did not achieve the specified intensifier pressure were re-expanded.

Based on the above, the existence of tube joints that may have been expanded at pressures slightly less than []^{a,c,e} in the WCGS steam generators is inherently factored into the pullout test results and, therefore, there is no effect on the H* distances that have been calculated in the report.

Addressing the B* distances provided in LTR-CDME-05-209-P, the leak rate testing was conducted based on test specimens that were manufactured using a specified expansion pressure of []^{a,c,e}. It has been verified that no tubes used in the original leak rate data analysis had expansion pressures of less than []^{a,c,e}. Regardless, the use of a lower bound expansion pressure for establishing primary-to-secondary leakage from the tube-to-tubesheet crevice is conservative.

5. *How does pressure and temperature cycling affect the pullout and leakage resistance of the joints? Cite the available data on this topic, and why it is appropriate that the proposed inspection depths need not specifically account for such cycling.*

Response

All of the full depth expansion processes used by Westinghouse close the gap between the tube and the tubesheet so that there is essentially no distance between these components. Therefore, the evaluation of effect of cyclic loading does not depend on the specific expansion process used. In an analysis for an F* plant (applicable to a hard-rolled expansion), the axial load to be applied to the sample for fatigue testing was calculated using both temperature and pressure components. Thermal loads were calculated assuming the tube became fixed at the top of the tubesheet due to crevice deposits at operating conditions. Upon shutdown, a tensile load is applied between the fixity locations due to differential thermal contraction. For pressure effects the tube was assumed to be loaded due to the end cap load at operating conditions, which is tensile, and the tensile load was maintained during shutdown conditions. The combined effects of pressure end cap loading and thermal growth were summed to determine the fatigue load to be applied for leak rate testing.

Among the samples leak tested prior to cycling, the average leak rate for all samples tested at 615 F at a pressure differential of 2650 was []^{a,c,e} The average leak rate of only those samples which leaked was []^{a,c,e} Following application of over 29000 fatigue cycles, the average leakage rate of the leaking specimens was []^{a,c,e} while the average of all samples was []^{a,c,e} (Reference 2). The consistency of these results suggests that the H* region will not be adversely affected by cycling/fatigue.

Based on this testing, Westinghouse concluded that there is no need for cyclic load testing for this type of configuration.

6. *Pullout resistance per unit length associated with the tube expansion process (residual pullout resistance) was determined on the basis of pullout tests and on the assumption that pullout resistance is uniform along the length of the joint. The axial force in the tube is maximum at the top of the tubesheet and decreases as joint friction incrementally picks up some of the load with increasing distance into the tubesheet. As axial force in the tube declines, with increasing distance in the tubesheet, the Poisson's contraction of the tube diameter decreases causing contact pressure to increase until it reaches a constant value at the location where axial force in the tube has been reduced to zero. At the pullout load, the pullout resistance per unit length near the bottom of the joint will be higher than the average pullout resistance along the entire joint. The pullout resistance over the upper portion of the joint will be less than the average resistance. Referring to Tables 7-6 to 7-10 in Enclosure 1, would not consideration of the actual distribution of the residual pullout resistance as a function of distance below the top of the tubesheet lead to larger H* values than shown on these Tables? If not, explain why not.*

Response

The use of the uniform pull out resistance is a conservative approximation. An incremental solution can be obtained by performing a numerical integration of the resistance force. An element of depth, dz , can

be analyzed as a linear approximation including an accounting for the Poisson contraction associated with the axial end cap force for that element. However, a key point to note is that it is not appropriate to actually use three times the axial force when the numerical integration is performed, because its use would result in three times the actual Poisson contraction. Instead, the actual axial force during NOp or SLB is used with the coefficient of friction divided by a factor of 3 or 1.4 respectively. For example, for the NOp calculations a coefficient of friction (μ) of []^{a,c,e} can be used to demonstrate a margin of 3 to the very conservative assumption of $\mu = 0.1$. While the numerical calculation is sensitive to the increment used, the sensitivity decreases with decreasing increment, an increment of []^{a,c,e} is sufficient (the estimated axial force decreases with increment, so using an increment of []^{a,c,e} is conservative). Since the increment is small, it is not necessary to incorporate the integration terms of the linearly increasing contact pressure with depth into the tubesheet. When such calculations are performed, it is found that the use of a constant contact pressure per unit length associated with the pullout force is conservative.

An example calculation was performed for the SLB case with a coefficient of friction of []^{a,c,e} by 1.4, with a resulting H^* value of 5.92 inches near the center of the tubesheet instead of the reported value of 6.34 inches. Similarly, H^* values at the periphery of the tubesheet were found to increase by about []^{a,c,e}

In summary, if the distribution of residual pullout force is used based on an integration of the incremental pullout resistance, the value of H^* was shown to decrease. Therefore the use of an average value of pullout resistance per unit length is conservative in that it yields a larger value for H^* .

7. *The models used to develop the H^* lengths are complex. Describe how these models have been verified to yield conservative H^* values. Have these models been verified by test? For example, how well do these models predict the actual residual pullout loads for joint test samples with typical H^* lengths (i.e., provide comparative data)?*

Response

The derivation of the model used to develop the H^* lengths was first documented in Appendix B of WCAP-15932 (for Callaway), it was also included in WCAP-16124 for WCGS. The derivation is an application of the Theory of Elasticity that was published by J. Goodier in the Transactions of the ASME in 1943. The numerical integration procedure described in the response to RAI #5 was used to verify the results of the use of the calculus to obtain the Theory of Elasticity solution. The model has been employed since the development of F^* in 1985, e.g., WCAP-11224 for the McGuire Model D steam generators, where it was used to verify the conservatism of the coefficient of friction used for the pullout calculations based on pullout and blowout test data. The model was used for the Model F calculations to estimate the contact pressure later used in the joint strength calculations.

The model used to develop the H^* depth is based on a combination of tube pullout test results and analysis. There are four source terms that must be considered relative to the determination of the interface pressure between the tube and the tubesheet. These source terms are:

1. the initial preload of the installation of the tube

2. internal pressure in the tube that is transmitted from the ID to the OD of the tube
3. thermal expansion of the tube relative to the tubesheet, and
4. bowing of the tubesheet that results in the dilation (above the center plane of the tubesheet) of the tubesheet holes

Two of the four effects on tube pullout strength have been measured: 1) The initial preload of the installation of the tube and 2) the thermal effect.

1. Preload from Expansion

The initial preload from the plastic deformation of the tube material due to hydraulic expansion does not result in a high contact pressure. However, it does provide a significant contribution to pullout force due to geometrical (mechanical) interlocking and surface roughness effects (Reference 18).

2. Differential Thermal Expansion

Table 2.0 summarizes the pullout test data for 0.75 inch diameter x 0.043 inch wall thickness tube specimens at several different temperatures. The data show that, for a short expansion length of 2.95 inches, the effective residual strength of the joint alone (at 70°F) coupled with the temperature effect (>70 °F) provides significant increase in pullout force. The joint strength would be expected to be approximately the same for similar expansion lengths in 0.6875 x 0.040 inch wall thickness tubes. For Model F steam generator tubing (1 1/16 inch diameter), []^{a,c,e} expansion lengths have been tested for the size resulting in similar trends.

The resulting pullout force at temperature provides more than ample margin to resist tube pullout resulting from end cap loads on a tube equivalent to either 3 times normal operating pressure differential (1680.3 lbf) or 1.4 times SLB pressure differential (1391 lbf) for the WCGS Unit 1 steam generators.

Table 2.0: Model D5 Pullout Test Data Sample (0.75 inch Diameter x 0.043 Inch Wall Thickness)

a,c,e

The effects of tube internal pressure and tubesheet bow on contact pressure have only been determined analytically. Of these, only tubesheet bow can have a potentially adverse effect on contact pressure and result in an increased H* distance since the loads imposed on the tube as a result of tubesheet bowing vary under various pressure and temperature conditions. The finite element analysis of the Model F tubesheet, channelhead, and lower shell was performed to determine the unit displacements throughout the tubesheet for two pressure unit loads (primary and secondary sides) and three thermal unit loads (tubesheet, shell and channelhead). The analysis yielded the unit displacements throughout the tubesheet for these five unit loads. The normal operating and faulted conditions (pressure and temperature) were then applied to these unit displacements to obtain the actual displacements for calculating the tube-to-tubesheet contact pressure distribution from the top to the bottom of the tubesheet.

The maximum and minimum values, as well as the limiting locations, for tubesheet bowing occur during the SLB condition. The maximum value is []^{a,c,e} at a radius of 3 inches from the centerline of the tubesheet. The minimum value is []^{a,c,e} at a radius of 60.2 inches from the centerline of the tubesheet. The maximum and minimum values of tubesheet bore expansion are expressed as the final radial gap values between the tube OD and tubesheet hole ID at the top of the tubesheet. The maximum radial gap value is []^{a,c,e} during a SLB condition.

As is common for most complex finite element analyses, the model employed in the determination of the H* distance has not been specifically benchmarked to test results. However, modeling methods are based

on accepted conservative analysis standards. For example, the perforated region of the tubesheet has been modeled as an equivalent solid plate based on the equivalent elastic constant equations for a square penetration pattern using an accepted modeling technique that has been used in a number of industries ("Stress Analysis of Thick Perforated Plates," PhD Thesis by T. Slot, Technomic Publishing Company, Westport, CN 1972). This equivalent solid plate, along with the other elements for the channelhead, tubesheet, and shell were modeled in the finite element program, WECAN/Plus, which has been QA verified for use in the Westinghouse organization.

The analysis model used to demonstrate that end cap loads for Normal and Faulted conditions are not transmitted below the H^* distance is described in Reference 3.

8. *Enclosure 1, Section 6.2.2 - The section states that room temperature leakage tests were performed on all test specimens at test pressures of 1900, 2650, and 3100 pounds per square inch (psi) (presumably applied on the primary side with nothing more than atmospheric pressure at the top of the joint). However, Table 6-2 only presents room temperature data for a differential pressure of 1000 psi. Where is this latter data discussed? Why aren't the room temperature data for the tests described in Section 6.2.2 included in Table 6-2 and Figure 6-6?*

Response

The presumption in the question that the secondary side pressure at the top of the tested joints was at atmospheric pressure is correct. This presumption is correct for the Model F test specimens.

The room temperature (RT) leak data shows that leak rate was essentially unchanged over the range of 1900 to 3100 psi. Associated contact pressures were only about 2000 psi. When the same samples are tested at 600F the contact pressures go up and leak rates go down, thus giving larger loss coefficients which are then not compatible with the RT data. This is why the 70F/1000 psi data is used only to anchor the 600F data at lower contact pressures. Using the 70F/1000 psi case results in a much more conservative relation of contact pressure and loss coefficient. If for example you use the 70F/1900 psi data, the slope of the regression increases for increasing contact pressure.

9. *Enclosure 1, Section 6.2.2-1 - The section states that the elevated temperature tests were performed following the room temperature tests. Section 6.2.2-2. states that the room temperature tests were performed following the elevated temperature tests. Please clarify this discrepancy.*

Response

The elevated temperature tests were performed after the room temperature tests (Reference 20).

10. Enclosure 1, Section 6.2.2-2 - The section states that a 1900 psi test pressure was used (simulating normal operating pressure) to keep the pressurizing fluid above saturation pressure. As the staff understands the report, the pressure at the upper end of the test joint is at atmospheric pressure which is not prototypic for normal operating conditions. As the test leakage goes from the bottom of the joint to the top, pressure at some point drops to less than saturation. Why would the test be expected to show as much leakage through the joint as would be the case under prototypic normal operating conditions?

Response

Note: This question is based on the information in LTR-CDME-05-209-P. Since this question was asked, data on the pressure in the crevice has become available. This data and the analytical treatment of the results of the test were provided to the NRC via a “White Paper” (LTR-SGDA-07-4 – included as Appendix A to this report). The following response is based on this recent data.

It has been shown by experiment that, for most of the distance through the tubesheet, the crevice pressure does not drop to below saturation pressure for large cracks in series with a crevice. The 1900 psi test pressure would be expected to result in less leakage because the test pressure is lower than the primary pressure during normal operating conditions of 2235 psig. The secondary side pressure does not significantly influence the crevice pressure.

There are two possible bases for determining which pressure to use during specific operating conditions: empirical test data and conservative assumptions based on engineering judgment. The empirical test data collected during tests performed on a simulated tubesheet collar with a hydraulically expanded tube consisted of measuring the pressure in-between the tube wall and the inner collar surface. The tube had six [

] ^{a,c,e} The purpose of the hole positioning and geometry was to eliminate any geometry based flaw effects. The results of the tests for steam line break (SLB) and normal operating (NOP) conditions are described in detail in the White Paper submitted to the NRC under docket numbers STN 50- 454, 50-455, 50-546, and 50-547. The results from the White Paper show that a limiting crevice pressure can be defined as a fraction of the primary side pressure for both SLB and NOP. The specific fractions, denoted as crevice pressure ratios in the White Paper, are [

] ^{a,c,e} The crevice pressure is determined by taking the primary pressure and multiplying by the appropriate crevice pressure ratio. For example, a NOP primary pressure of 2250 psi would result in a crevice pressure of [

] ^{a,c,e} Similarly, the crevice pressure for a primary pressure of 2560 psi during SLB results in a crevice pressure of approximately [

] ^{a,c,e} The leak rate is directly proportional to the pressure drop across the tube wall into the crevice. The pressure drop across the tube wall during NOP is 2250 psi minus [

] ^{a,c,e} The pressure drop from the example SLB condition is 2560 psi minus [

] ^{a,c,e} The change in driving head on any leaked fluid, combined with the change in contact pressure due to the increased pressure in the tube/tubesheet crevice, still results in a leak rate ratio, defined as the leakage during SLB divided by the leakage during NOP, of less than two.

The crevice pressure interpretation in the White Paper is conservative and focuses on the largest differences in operating conditions and how to apply them in a fashion that has the greatest impact on contact pressure. Another conclusion that is equally supported by the test data is that different crevice pressure ratios can be used that show that the leak rate would either not increase, or would potentially decrease, during accident conditions. For instance, in the White Paper, if the median is used to calculate the crevice pressure ratios from the total set of all available test data then ratios of []^{a,c,e} are obtained for NOP and SLB conditions, respectively. Using those values to determine the pressure in the crevice gives a pressure drop across the tube wall of approximately []^{a,c,e} during NOP and SLB conditions, respectively. The difference between the pressure drop for NOP and SLB using the total set median values is approximately []^{a,c,e}. Such a small difference in driving pressure on the leak, combined with the change in temperature and tubesheet bow during accident conditions, reduce the leak rate during a SLB so that the leakage during NOP is []^{a,c,e}.

In smaller cracks, it is possible for geometry based effects to change the way that the pressure develops in the tube/tubesheet crevice. In such a case, the pressure in the crevice may be much lower than suggested by the test results reported in the White Paper. In that event, the assumption of secondary side pressure in the crevice is conservative during both NOP and SLB conditions. In the case of NOP, the lower the pressure in the crevice the greater the pressure drop across the tube wall. For example, assuming a secondary side pressure of 750 psi in the crevice during NOP results in a pressure drop of 2250 psi minus 750 psi which equals 1500 psi. Similarly, assuming the secondary pressure in the crevice during SLB conditions results in a pressure drop of 2560 psi (assuming 0 psi secondary side pressure during an SLB event). The difference between the drop in pressure during the NOP and SLB conditions is 1060 psi and results in a SLB to NOP leak rate ratio of less than two. If the crevice pressure during NOP was lower than the secondary side pressure, say that it was equal to 0 psi, then the pressure drop across the tube wall during NOP would be equal to 2250 psi. The difference between the drop in pressure during the NOP and SLB conditions would then become 310 psi. The leak rate ratio between the NOP and SLB conditions, with a much smaller difference in the driving head on the leakage between NOP and SLB, would be much less than two.

11. The plot of Model F loss coefficient versus contact pressure in Figure 6-6 of Enclosure 1 exhibits a higher slope than is the case for Model D5. The difference appears attributable to lower loss coefficients at lower contact pressures for Model F than for Model D5. Discuss the differences between the Model F and D5 SG designs that explain their different behaviors. If no significant design differences can be identified, discuss the credibility of the loss coefficient data.

Response

There are no design differences, other than tube diameter, between the Model F SGs and the Model D5 SGs that would be expected to lead to significantly different results in the loss coefficient data. However, further examination of the test results from both the Model F and the Model D5 provide a potential explanation of the different results. Also, the impact of the new crevice pressure data (Ref: White Paper) provide a different interpretation of the loss coefficient data. Since there are no significant design differences, and both data sets can be reasonably expected to represent the physical effects, combination of the data sets is appropriate.

Test results from Model F specimens that were not prepared in accordance with criteria of the test specifications (e.g. expansion pressures for the tubes were below []^{a,c,e}) were removed from consideration as usable test results. Similarly, for the Model D data, test results that did not support the test objectives of leakage, such as a result of no leakage, were removed from consideration as a usable test result. The net effect of these data exclusions on the data population of the Model F and Model D results was:

1. To decrease the variability of the Model D data and exclude the higher loss coefficient results.
2. To increase the variability of the Model F data and exclude the low loss coefficient results.

Figure 11 is a plot of the combined Model D and Model F total data set. Figure 12 shows a plot of the total Model D, total Model F and combined data set log normal linear regression model fits using the assumptions discussed in LTR-CDME-05-209-P. In this context, the term “total” means that all available data for each type of specimen was used in the regression analysis and no test data were excluded. The assumptions discussed in LTR-CDME-05-209-P include: flashing in the crevice, no change in pressure differential calculations due to crevice pressure, the Model F results scaled to compare to Model D results on the basis of tube diameter and all contact pressures calculated using the same theory of elasticity model.

a,c,e



Figure 11: Plot of Model D and Model F Total Data Set for 70 °F and 600 °F Conditions

a,c,e



Figure 12: Total Data Set Fit Using Original Assumptions

The data in Figure 11 and Figure 12 show that the average loss coefficient for the Model D is much higher than the average loss coefficient for the Model F. The combined loss coefficient fit curve splits the difference between the Model F and Model D data.

Figure 13 shows a plot of the log normal linear regression model results using the total Model F and Model D data set and incorporating the results of the crevice pressure study reported in the White Paper. When all of the data from both sets of experiments are included, and the contact pressures during the applied pressure differentials are re-calculated to reflect the results of the crevice pressure tests (Appendix A), the means of the regression fits of the two populations become very similar. Therefore, it can be concluded that the difference between the Model D5 tests and the model F tests lies in normal variation of test specimens, test control, etc.

Figure 14 is a plot of the 95% confidence limit log normal linear regression model results using the total Model F and Model D data set and incorporating the results of the crevice pressure study reported in the White Paper. The 95% confidence limit fit of the total set of the Model F and Model D data results in a correlation between loss coefficient and contact pressure with a positive slope.

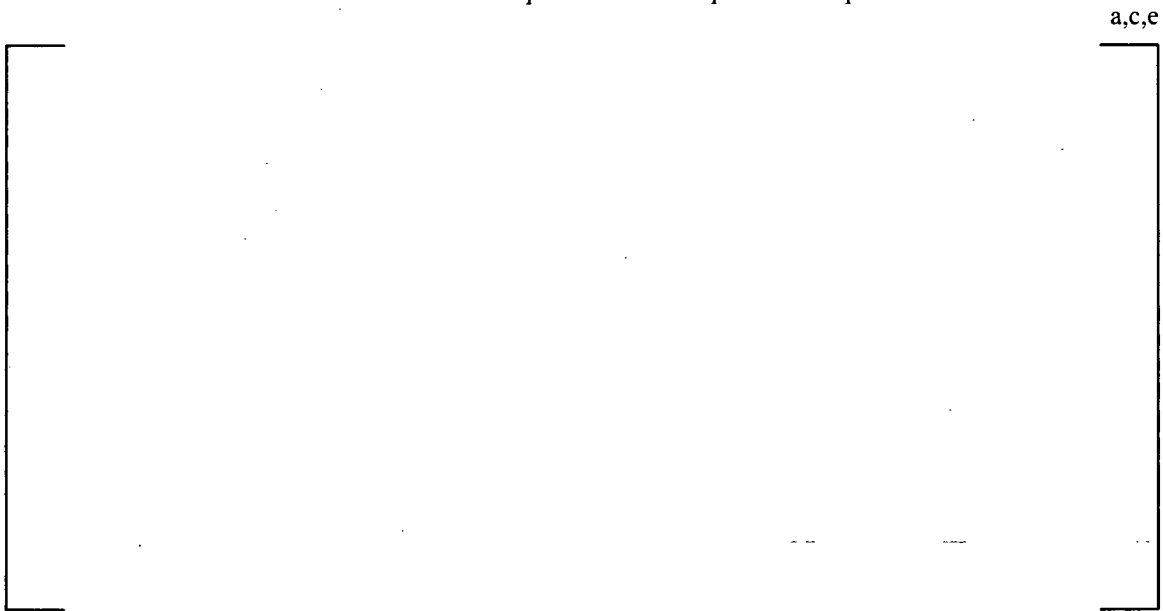


Figure 13: No Flashing in the Crevice, Crevice Pressure Varied based on applied ΔP , Scaled Total Data Set Results



Figure 14: 95% Confidence Limit Results for Varied Crevice Pressure, Total Data Set and No Flashing in the Crevice

The Model F data is more variable than the Model D and skewed toward the upper end of the data population. The Model D data is less variable than the Model F and clustered around the lower end of the data population. When combined, the total data set supports a positive relationship between loss coefficient and contact pressure and confirms the conclusion of LTR-CDME- 05-209-P.

If the most conservative loss coefficient versus contact pressure model is used, shown in Figure 14 as the 95% confidence limit fit of the combined data sets, the conclusions of the B* analysis do not change. The summary plots for the H* and B* analysis shown below (Figure 15 and 16) prove that the leak rate ratio between SLB and NOP does not exceed a value of 2 regardless of whether the original loss coefficient or modified loss coefficient model is used. The B* distances calculated using the original loss coefficient assumptions and the updated results are shown in Figure 15 and 16 (Reference 7).

The effect of considering no relationship, or a zero slope model, between contact pressure and loss coefficient was also considered in this analysis. Assuming a constant value for the loss coefficient negates any benefit from loss coefficient data and forces the leak rate resistance to be calculated based on the effect of the tubesheet bow and potential flow area in the crevice. Two constant loss coefficient values were compared in this analysis:

1. The lowest possible value from the 95% confidence fit of the Model D data, $k = [\quad]^{a,c,e}$
2. The mean of the total combined Model D and Model F data set, assuming flashing in the crevice, $k = [\quad]^{a,c,e}$

The net effect of assuming a constant loss coefficient value, and reduced contact pressure, is to increase the maximum B* depth by approximately 0.50 inch over the values plotted in Figure 16. If the lower loss coefficient value is assumed to be constant, then the maximum B* depth increases by slightly more than

0.50 inch. If the mean loss coefficient value is assumed to be constant, then the maximum B* depth increases by slightly less than 0.50 inch (Reference 7).

a,c,e



Figure 15: Summary Plot of H*/B* Results Using the Original Loss Coefficient Model, DP = 0.76, No Crevice Pressure Modifications and Residual Mechanical Strength in the Joint During SLB



Figure 16: Summary Plot of H^*/B^* Results, $DP = 1.0$, No Residual Mechanical Strength in the Joint During SLB and Using the 95% Confidence Fit of the Loss Coefficient Model for the Total Model F and Model D Data Set (assuming varied crevice pressure results and no flashing in the crevice)

12. Enclosure 1, Section 6.2.2.1 - The section states that the leak test results averaged 16 drops per minute (dpm) per joint at 1900 psi compared to 59 dpm at higher pressures. This is a factor of 3.7 difference. Discuss why this difference is so high compared to the factor of 2 which, under the bellwether principle, is assumed to bound the increase in leakage going from normal operating to accident conditions.

Response

The average leakage rate reported in LTR-CDME-05-209-P was reviewed and has been determined to be incorrect. The average leak rate for the different leak rate test conditions at an elevated temperature of 600 F for a []^{a,c,e} diameter tubesheet hole are included in the following table. Leak rate is shown to decrease with increasing test pressure differential (Reference 8).

Leak Rate Test Pressure (psi)	Measured Leak Rate (drops per minute at room temperature)

a,c,e

13. Enclosure 1, Section 7.1.2, page 45 of 127: Was the primary pressure unit load applied only to the primary face of the tubesheet, and not to the side of the tubesheet bore holes? Was the secondary pressure unit load applied only to the secondary face of the tubesheet, and not to the side of the tubesheet bore holes? Was the tube end cap pressure load (due to primary and secondary pressures) included in the finite element analyses?

Response

The finite element analysis used an anisotropic material model to represent the perforated region of the tubesheet without requiring the modeling of the individual perforations in the tubesheet. The model does not discretely model each hole, but models the materials and geometric effects of the holes through the use of an equivalence technique. The specific method used to represent the tubesheet is described by Slot (Reference 9). The results of the finite element analysis determine the bow of the tubesheet and the accompanying radial displacements as a function of location in the tubesheet (i.e., depth and radius). The equations described in LTR-CDME-05-209-P are then used to combine the results of the internal and external loadings with the finite element analysis on the tubes and tubesheet holes to produce the final contact pressure estimates.

Because the finite element model utilizes an anisotropic material model to represent the perforated plate, it is not necessary to apply the primary or secondary pressure unit loads to the bore holes. The primary and secondary pressures were only applied to their respective tubesheet faces in the finite element analysis. The tube end cap pressure load was not included in the finite element analyses but is included in

the subsequent analysis of the results in determining the amount of tube dilation and its contribution to the contact pressure.

14. Enclosure 1, Section 7.1.2, page 45 of 127: The 500 °F unit loads represent which of the following; heating up from 70 to 500 °F, or from 70 to 570 °F? If the former, why isn't 70 °F subtracted from 500 °F in the radial deflection scaling factors in Section 7.1.3 (page 46 of 127)?

Response

The unit load cases consider an increase in the temperature of 500°F, i.e., from 70 to 570°F, so the calculations for the actual conditions are based on temperature changes relative to 70°F.

15. Enclosure 1: Regarding the equation for ΔR_{TS}^{Pr} top of page 48 of 127, should not P_i be P_o consistent with the last equation appearing on page 48? If not, why not?

Response

The choice of which pressure term is used is a matter of which element is being considered relative to the application of the pressure. For example, P_i is applied to the ID of the tubesheet hole, but is also applied to the OD of the tube as P_o . The wording on page 48 should be changed to read:

The thermal expansion of the hole ID is included in the finite element results and does not have to be expressly considered in the algebra; however, the expansion of the hole ID produced by pressure is given by:

$$\left[\frac{P_i d^3}{E_{TS} (1 - \nu^2)} \right]^{a,c,e}$$

Where: E_{TS} = Modulus of Elasticity of Tubesheet, psi

d = Outside radius of cylinder which provides the same radial stiffness as the tubesheet, that is []^{a,c,e}

Note that in this context the P_i term represents the pressure applied to the ID of the tubesheet hole and to the OD of the tube.

16. Enclosure 1, Section 7.1.3 - The tube inside and outside radii within the tubesheet after expansion shown on page 49 of 127 appear not to be entirely consistent with the numbers on page 44 of 127. Explain this inconsistency or, alternatively, show that this inconsistency does not significantly affect the outcome of the overall analysis.

Response

The correct dimensions for the inside and outside radii of the tubes have been used in the analysis. The inside radius of the tubes used in the analysis is []^{a,c,e} The outside radius of the tubes used in

the analysis is []^{a,c,e} The inconsistency is an artifact of working on documents for SGs with 0.750 inch diameter tubes and 0.688 inch diameter tubes in the same timeframe.

17. Enclosure 1, Section 7.1.4 - Near the top of page 50 of 127, it is stated that the secondary pressure is conservatively assumed to act on the outside of the tube and the inside of the tubesheet hole. The staff agrees that this is conservative from the standpoint of maximizing leakage under normal operating conditions, but is concerned that it may be non-conservative from the standpoint of determining conservative ratios of accident leakage to normal operating leakage. Wouldn't the assumption of no secondary pressure yield a lesser value of normal operating leakage, leading to a higher ratio of accident to normal operating leakage? What is the basis for describing the assumption on secondary pressure as conservative?

Response

Note: This question is based on the information in LTR-CDME-05-209-P. Since the issue date of this RAI, new data on the pressure in the crevice has become available. In addition, the issue of divider plate integrity has been raised (see RAI # 25), and this question plays an integral role in the analysis for H*/B*. This data and the analytical treatment of the results of the test, and consideration of divider plate effectiveness were provided to the NRC via a "White Paper" (Appendix A of this report). Because the new crevice pressure test data invalidates the original assumption of the crevice pressure being at the secondary side pressure, the RAI as stated does not apply specifically to the revised calculation basis. The following response is based on this recent data and integral modeling of the divider plate and is a best effort to address the question as it may apply to the revised analysis.

As noted above in the response to NRC RAI # 10, based on Reference 10 it has been determined in tests that the pressure in the crevice of the tubesheet remains above the saturation pressure along the entire length of the crevice in the test specimens during normal operating conditions and postulated steam line break conditions. The pressure in the crevice under NOp and SLB is sufficiently high to keep the fluid single phase in the entire crevice up to nearly the top of the test specimen. The H*/B* analyses provided in LTR-CDME-05-209-P assumed that the full secondary side pressure at each respective condition was present in the crevice due to the assumption that the liquid would flash to steam outside the postulated flaw. The new data discussed in Reference 10 invalidates this assumption. For the WCGS steam generators, it is concluded in Reference 10 that the crevice pressure during normal operating conditions will remain at a constant value of []^{a,c,e} During a postulated SLB event, the crevice pressure is determined to remain at a value of []^{a,c,e}

A revised analysis of the B*/H* values utilizing the new crevice pressure test data has been completed. The revised analysis results, for three different cases, are provided in Table 3.0 below. The Case 1 results shown in Table 3.0 are for the limiting Cold Leg analysis and include the following assumptions:

- Although the pullout test data indicated positive residual mechanical joint strength, the residual joint strength is ignored for SLB accident condition to conservatively account for postulated variability of the coefficient of thermal expansion.
- No vertical restraint from the divider plate (DP = 1.00).
- Increased crevice pressures consistent with the analysis presented in Appendix A.

- Use of the lower 95% confidence interval fit of the combined Model F and Model D total data set of leak rate testing.

The Case 2 results are also for the limiting Cold Leg analysis but they include the assumption of a fully functional divider plate []^{a,c,e} All of the other assumptions for Case 2 are the same as for Case 1.

The Case 3 results show the maximum H* and B* depths for the analysis under the original assumptions stated in LTR-CDME-05-209-P.

Table 3.0: Maximum H*/B* Result (the reference for H* and B* is the top of the tubesheet)		
Case	B* (in)	H* (in)
1	9.37	11.37
2	3.00	4.84
3**	4.79 (5.4)	7.06 (6.9)

** For Case 3, the numbers in parentheses correspond to the original results included in LTR-CDME-05-209-P. These numbers have since been revised to reflect updated analysis results.

In summary:

1. The underlying assumptions for the crevice pressure have been changed by the new test data for crevice pressure which shows that the pressure in the crevice is essentially at the primary side pressure for most of the length of the crevice in the test specimens. Since the crevice pressure is no longer assumed to be equal to the secondary side pressure, the basis for the RAI does not appear to exist any more.
2. Analyses based on the revised pressure model for the crevice, based on the new test data, and assuming both a fully functional and fully non-functional divider plate, and also assuming that no residual joint strength is provided by the tubesheet expansion process show that B* is bounded by H* in every case. The definition of B* is the depth into the tubesheet at which the ratio of leakage at SLB conditions is twice that at NOp conditions.

Tables 7-6 through 7-12, Figures 7-3 through 7-6, and Figures 8-1 through 8-6 of LTR-CDME-05-209-P have been revised to reflect the new crevice pressure data and analyses and to reflect a divider plate which is assumed to be non-functional and are provided below. Note that in this context the term “non-functional” refers only to the ability of the divider plate to restrict vertical displacements of the tubesheet. Crevice pressure ratios of []^{a,c,e} were used to implement the new pressure test data for

the steam line break and normal operating conditions, respectively. A divider plate factor of 1.00 is used to eliminate any restraint of the vertical tubesheet displacements. Similar information is provided for both the hot leg and the cold leg. The revised tables and figures for the hot leg are provided first followed by the same tables and figures for the cold leg.

HOT LEG RESULTS

Table 7-6. Cumulative Forces Resisting Pull Out from the TTS Wolf Creek
Hot Leg Normal Conditions – Reduced T_{hot} , $P_{sec} = 792$ psig

a,c,e

Table 7-12. H* Summary Table Structural Criteria Required Engagement		
Zone	Limiting Loading Condition	Engagement from TTS (inches)
		Hot Leg
A	$1.4 \cdot \Delta P_{FLB}^{(1,2)}$	3.15 ⁽³⁾
B	$3 \cdot \Delta P_{NOp}^{(1,2)}$	9.47 ⁽³⁾
C	$3 \cdot \Delta P_{NOp}^{(1,2)}$	10.55 ⁽³⁾
D	$3 \cdot \Delta P_{NOp}^{(1,2)}$	10.54 ⁽³⁾

Notes:

1. Seismic loads have been considered and are not significant in the tube joint region (Reference 12).
2. The scenario of tubes locked at support plates is not considered to be a credible event in Model F SGs as they are manufactured with stainless steel support plates. However, conservatively assuming that the tubes become locked at 100% power conditions, the maximum force induced in an active tube as the SG cools to room temperature is [$\gamma^{a,c,e}$]
3. 0.3 inches was added to the H* values to account for the BET location relative to the TTS.
4. $1.4 \cdot \Delta P_{FLB}$ conditions.
5. B* requirements for leak rate are provided in Table 9-2.

a,c,e



Figure 7-3. Contact Pressures for NOP at Wolf Creek, Reduced T_{hot} , $P_{sec} = 792$ psig

a,c,e



Figure 7-4. Contact Pressures for NOP at Wolf Creek, $T_{hot} = 620^{\circ}\text{F}$, $P_{sec} = 935$ psig



Figure 7-5. Contact Pressures for SLB Faulted Condition at Wolf Creek

a,c,e

Figure 7-6. Contact Pressures for FLB Condition at Wolf Creek, Reduced T_{hot}

a,c,e

Figure 7-7. Contact Pressures for FLB Condition at Wolf Creek, $T_{hot} = 620$ F

a,c,e

Figure 8-1. Change in Contact Pressure at 20.0 Inches Below the TTS

a,c,e

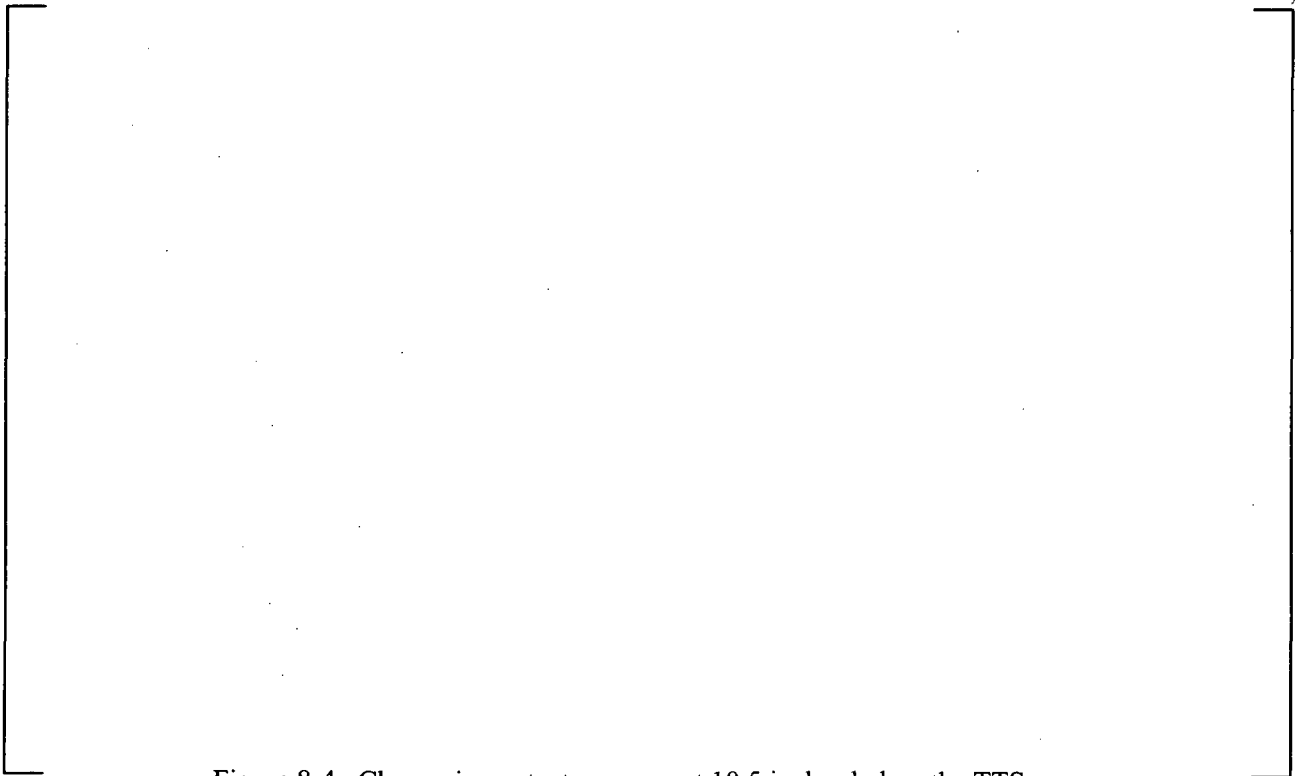


Figure 8-2. Change in Contact Pressure at 16.9 Inches Below the TTS

a,c,e

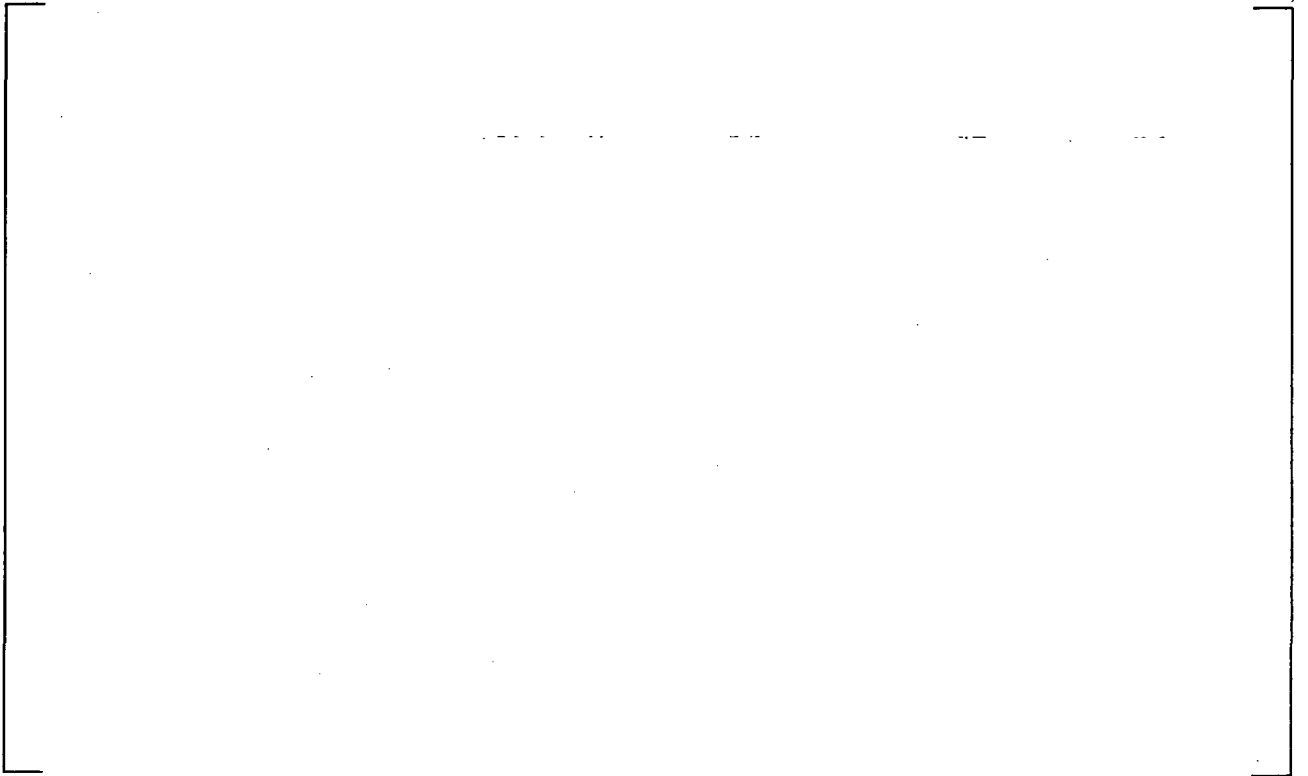


Figure 8-3. Change in Contact Pressure at 12.6 Inches Below the TTS



a,c,e

Figure 8-4. Change in contact pressure at 10.5 inches below the TTS



a,c,e

Figure 8-5. Change in Contact Pressure at 8.25 Inches Below the TTS



Figure 8-6. Change in Contact Pressure at 6.0 Inches Below the TTS



Figure 11-1. Comparison of H* and B* Hot Leg Results

COLD LEG RESULTS

Table 7-6a. Cumulative Forces Resisting Pull Out from the TTS Wolf Creek
Cold Leg Normal Conditions – Reduced T_{hot} , $P_{sec} = 792$ psig

a,c,e

Table 7-12a. H* Summary Table Structural Criteria Required Engagement		
Zone	Limiting Loading Condition	Engagement from TTS (inches)
		Cold Leg
A	$3 \cdot \Delta P_{Nop}^{(1,2)}$	4.56 ^(3,)
B	$3 \cdot \Delta P_{Nop}^{(1,2)}$	10.63 ⁽³⁾
C	$3 \cdot \Delta P_{Nop}^{(1,2)}$	11.37 ⁽³⁾
D	$3 \cdot \Delta P_{Nop}^{(1,2)}$	11.35 ⁽³⁾

Notes:

1. Seismic loads have been considered and are not significant in the tube joint region (Reference 12).
2. The scenario of tubes locked at support plates is not considered to be a credible event in Model F SGs as they are manufactured with stainless steel support plates. However, conservatively assuming that the tubes become locked at 100% power conditions, the maximum force induced in an active tube as the SG cools to room temperature is [$J^{a,c,e}$]
3. 0.3 inches was added to the H* values to account for the BET location relative to the TTS.

a,c,e



Figure 7-3a. Contact Pressures for Nop at Wolf Creek, Reduced T_{hot} , $P_{sec} = 792$ psig

a,c,e



Figure 7-4a. Contact Pressures for Nop at Wolf Creek, $T_{hot} = 620^{\circ}\text{F}$, $P_{sec} = 935$ psig



Figure 7-5a. Contact Pressures for SLB Faulted Condition at Wolf Creek

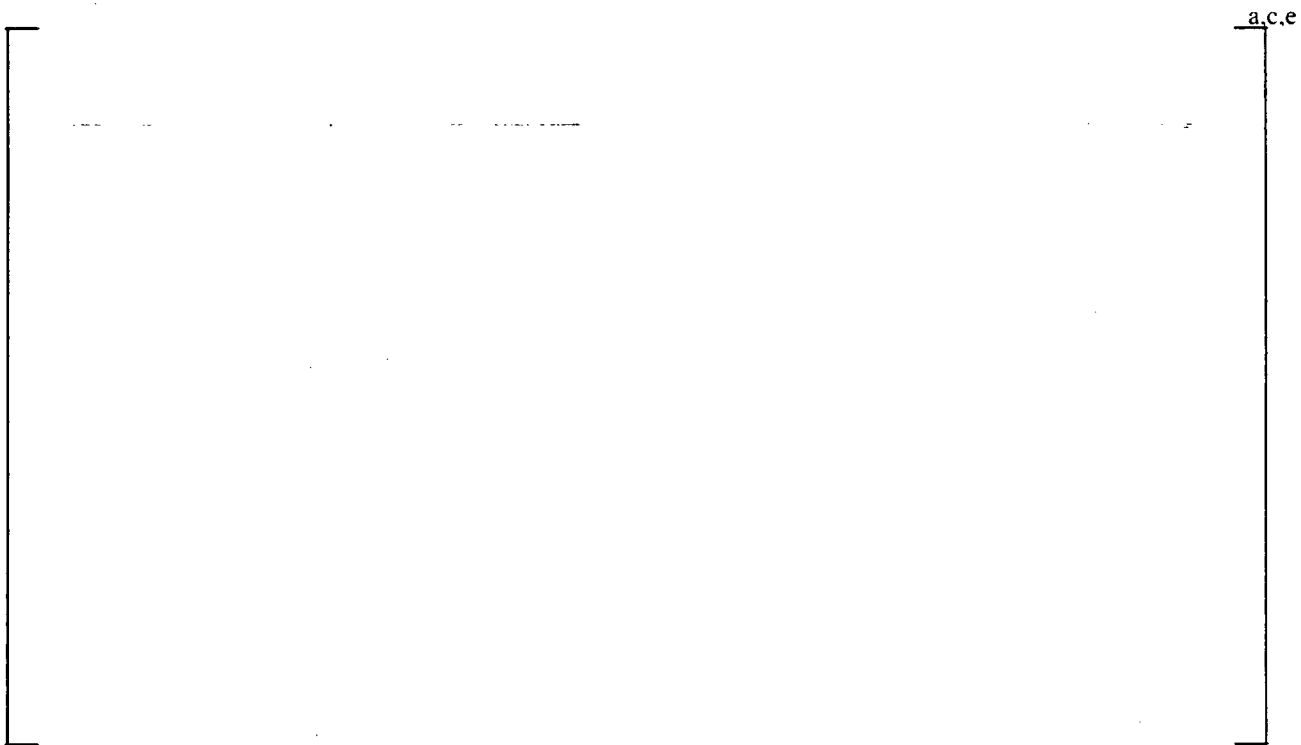


Figure 7-6a. Contact Pressures for FLB Condition at Wolf Creek, Reduced T_{hot}

7-7a. Contact Pressures for FLB Condition at Wolf Creek, $T_{hot} = 620$ F



Figure 8-1a. Change in Contact Pressure at 20.0 Inches Below the TTS

a,c,e



Figure 8-2a. Change in Contact Pressure at 16.9 Inches Below the TTS



Figure 8-3a. Change in Contact Pressure at 12.6 Inches Below the TTS



Figure 8-4a. Change in Contact Pressure at 10.5 Inches Below the TTS

a,c,e



Figure 8-5a. Change in Contact Pressure at 8.25 Inches Below the TTS

a.c.e

Figure 8-6a. Change in Contact Pressure at 6.0 Inches Below the TTS

a,c,e



Figure 11-2. Comparison of H* and B* Cold Leg Results

18. Enclosure 1, Section 8.2 - The ligament tearing discussion in Section 8.2 (starting on page 75 of 127) only addresses circumferential cracks. Please provide corresponding discussion for axial cracks.

Response

Axial ligament tearing may occur during a postulated accident when the differential pressure across the tube wall is significantly greater than during normal operation. Ligament tearing is accounted for in the strength evaluations that demonstrate a resistance to pullout in excess of $3\Delta P$ for normal operation and $1.4\Delta P$ for postulated accident conditions.

The tube area required to resist tearing due to an axially oriented crack can be calculated using traditional mechanics. It is conservative, in this case, to neglect the forces that would act to keep a crack closed and compress the flanks in the ligament so that tensile tearing would become unlikely. This includes the far field axial stress on the tube cross section generated by internal pressure end cap loads which would act to close the ligament and any cracks above the H^* depth. The axial orientation of the damage in the tube means that the required area of the tube cross section to resist tearing and damage should be based on the local strength of the material around the crack. This is in contrast to the typical method used to compare what percent of the area is required to resist ligament tearing in circumferentially damaged tubes based on the amount of force applied to the damaged tube cross section.

The allowable ratio of the applied stress on a tube cross section to the limiting stress the tube cross section can support may be defined as

$$n = \frac{\sigma_{APPLIED}}{\sigma_{LIMIT}} \quad (1)$$

where $\sigma_{APPLIED}$ is the stress applied to the cross section under either the normal operating condition or a steam line break and σ_{LIMIT} is either the ASME code minimum tensile yield stress of the tube material (used to predict yield in the ligament) or the ASME code minimum ultimate tensile strength of the tube (used to predict rupture and tearing of the ligament). The significant properties of the tube cross section are defined as

$$A_{INITIAL} = \pi(r_o^2 - r_i^2) \quad (2)$$

$$A_{MIN} = \pi(r_o^2 - r_{min,i}^2) \quad (3)$$

$$t = r_o - r_i \quad (4)$$

$$R_M = \frac{r_o + r_i}{2} \quad (5)$$

where $A_{INITIAL}$ is the cross sectional area of the tube in the undamaged state, A_{MIN} is the minimum cross sectional area required to resist ligament tearing, t is the thickness of the tube wall, R_M is the mean radius

of the tube, r_o is the outer radius, r_i is the initial inner tube radius and $r_{min,i}$ is the minimum inner radius of the tube in the damaged configuration that can still resist ligament tearing.

In the case of an axial crack, the largest local stress contributing to the damage in the tube is [the hoop stress acting on the tube due to the internal pressure. The hoop stress acting on the tube cross section is calculated using the following relationship

$$\sigma_{HOOP} = \frac{Pr}{t} = \frac{PR_M}{t} = \frac{SP_{LIMIT}R_M}{t} \quad (6)$$

Where S is the given safety factor used in the analysis for conservatism and P_{LIMIT} is the limiting internal pressure that will initiate tearing in the tube. The limiting state in the tube material where the ligament will still hold occurs when the applied loading is equal to the allowable loading that the damaged cross section can bear, or when $n = 1$, as shown below.

$$n = 1 = \frac{\sigma_{APPLIED}}{\sigma_{LIMIT}} \rightarrow \sigma_{LIMIT} = \sigma_{APPLIED} \quad (7)$$

The applied stress can be written as

$$\sigma_{APPLIED} = \frac{F_{LIMIT}}{A_{MIN}} \quad (8)$$

$$F_{LIMIT} = \sigma_{HOOP} A_{INITIAL} \quad (9)$$

where F_{LIMIT} is the force applied to the cross section by the limiting internal pressure. Substitution of Equations 7 and 9 into Equation 8, and rearranging to solve for A_{MIN} , gives

$$\sigma_{LIMIT} = \frac{\sigma_{HOOP}}{A_{MIN}} A_{INITIAL}$$

$$\sigma_{LIMIT} A_{MIN} = \sigma_{HOOP} A_{INITIAL} \rightarrow A_{MIN} = \frac{\sigma_{HOOP} A_{INITIAL}}{\sigma_{LIMIT}} \quad (10)$$

Substitution of the definitions for t , R_M , σ_{HOOP} and $A_{INITIAL}$ into the equation for A_{MIN} yields

$$A_{MIN} = \left(\frac{r_o + r_i}{2} \right) \left(\frac{1}{r_o - r_i} \right) \frac{SP_{LIMIT}}{\sigma_{LIMIT}} \pi (r_o^2 - r_i^2) \quad (11)$$

Substitution of Equation 3 into 11 and using the difference of squares identity to rearrange and solve for the minimum inside radius in the damaged tube gives the final result.

$$\left[\dots \right]^{a,c,e} \quad (12)$$

The results shown in the table below were obtained using the ASME code minimum material properties (Reference 11) and the physical parameters of the Model F steam generator tubes. The results from Equation 12 were compared to the method used to calculate the required thickness to resist ligament tearing due to circumferential cracking (Reference 12) and the method described in the EPRI Tube Integrity Theory Manual (Reference 13) and Reference 21. [

--	--

The results of the axial ligament tearing calculations detailed above are [

]^{a,c,e}

Considering the worst-case scenario, the likelihood of ligament tearing from axial cracks resulting from an accident pressure increase is [

]^{a,c,e} Therefore, the potential for axial ligament tearing is considered to be a secondary effect of essentially negligible probability and should not affect the results and conclusions reported for the H* evaluation. The leak rate model does not include provisions for predicting ligament tearing and subsequent leakage. Increasing the complexity of the model to attempt to account for axial or circumferential ligament tearing is not considered necessary.

19. *The structural and leakage assessments supporting the proposed technical specification amendment are for tubes with no degradation in the proposed inspection zone. The proposed inspection depths make no allowance for degradation which may occur within this zone prior to the next scheduled inspection. Assess the potential impact of degradation in the inspection zone on (1) contact pressures between the tube and tubesheet, (2) on tube pullout capacity, and (3) on leakage under normal and accident conditions. (Although flaws in this zone will be plugged on*

detection, this question is relevant to satisfying the tube integrity performance criteria with respect to condition monitoring and operational assessments.) This assessment should address potential axial and circumferential stress corrosion cracks (SCC) and volumetric intergranular attack (IGA) flaws.

Response

PWSCC was reported at Catawba Unit 2 (October 2004) and Vogtle Unit 1 (March 2005), both plants with A600 TT tubing. Pre-outage screening for expansion zone anomalies was performed to identify the population in two categories: 1) bulges, identified in the screening process as BLG and characterized by a bobbin voltage, and 2) over expansions, identified in the screening process as OXP and characterized by a deviation from the mean tubesheet expanded diameter and a minimum length. (The BLG and OXP names are used for convenience in the screening process and are not the same BLG and OXP indications recorded during the inspection.)

A sampling program that included greater than 50% of the combined population of bulges (BLG) and over-expansions (OXP) in the tubesheet region from the top of the tubesheet to minus 17 inches from the pre-outage screening process was performed during Refueling Outage 15 in the WCGS steam generators A and D (sample inspection also performed in SG B and C during Refueling Outage 14). Based on first principles and current operating experience, it is not possible to associate the potential for crack initiation with the characteristics of the BLG and OXP signals from the previous screening process. However, the sample selected included a wide range of BLG voltages and OXP dimension. The sample was concentrated in the region from top of the tubesheet to top of the tubesheet-10 inches since this region represents the most safety significant region of the tubesheet expansion region.

No indications of cracking were reported from the 50% sample program for the tubesheet expansion region BLG and OXP as defined by the pre-outage screening criteria. Therefore, no structural or leakage concerns would be expected during subsequent operation of WCGS Unit 1.

The potential impact of the occurrence of degradation in the future can be addressed by reviewing the occurrence of cracking in mill annealed tubing steam generator tube joints. The available data for the population of circumferential cracks are from the 1999 inspection record of the circumferential cracks at Callaway Unit 1 in mill-annealed Alloy 600 tubing. The tubing in the Wolf Creek Unit 1 steam generators is made from Alloy 600TT, which is significantly less sensitive to cracking initiation and propagation than the mill annealed tubing.

The available data were provided in WCAP-15932 (Reference 3), the Callaway docket, NRC Accession No. ML022910436. The total data set included 40 circumferential cracks observed, with an average crack angle of $40.18^\circ \pm 21.62^\circ$, a maximum angle of 108° and a minimum angle of 20° . Of this population, 87.5% of the cracks were less than 0.5 inch in arc length, and 75% of the cracks covered an angle of 40° or less. In the data set, 25% of the circumferential cracks were 95% through wall or greater; only a single crack was identified as 100% through wall. The depths of the indications were consistent with the data from prior inspections and suggest very little crack depth growth occurred.

For a tube with a 0.688 inch outer diameter (Model F steam generator), a crack angle of 40° corresponds to a crack arc length of approximately 0.24 inches. From a structural/tube pullout capability perspective,

as reported in LTR-CDME-05-209-P, even if the expansion joint were not present, tubes with circumferential cracks up to about 180° have sufficient strength to meet the nominal ASME Code structural requirements.

The predicted crack opening area for a guided circumferential crack (constrained from bending, crack opening constrained above the H* depth) 0.24 inch in length, using the models described in WCAP-15932 and illustrated in Figure 17, is approximately 7.5e-6 in² for the NOp condition and 1.8e-5 in² for the SLB condition. These crack opening areas are reduced by an order of magnitude, roughly, for distances below the H* depth.

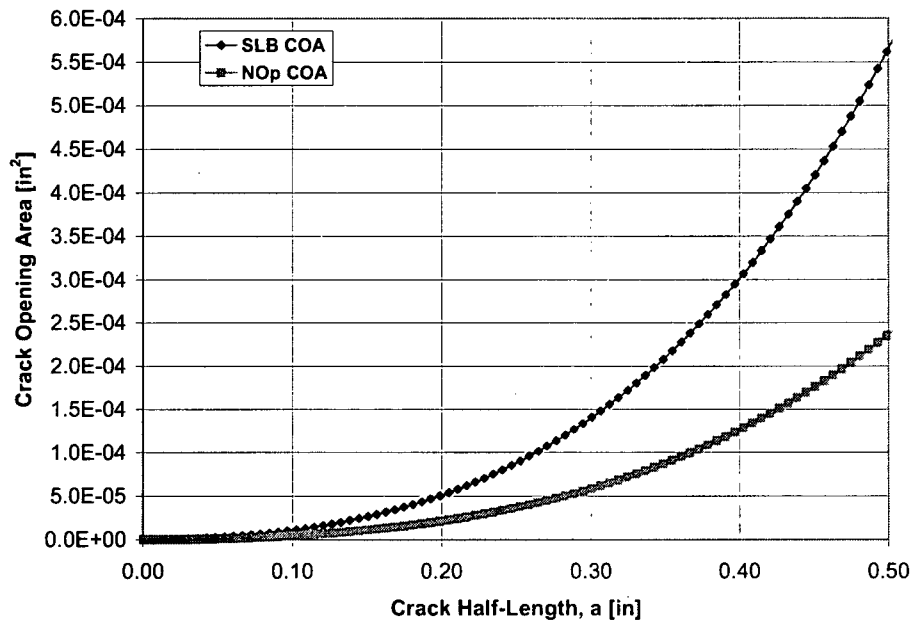


Figure 17: Plot of Guided Circumferential Crack Opening Area for a Model F SG

It is reasonable to consider a value for crack opening area on the order of 10⁻⁵ in², or less, as negligible. This conclusion is consistent with the values for crack opening area that can be calculated using the alternate approach of calculating the kink angle compatibility via methods described in The Stress Analysis of Cracks Handbook (2nd Edition) by Tada. The result of such calculations, given in case 33.1 and 33.2 of the text, show that the crack opening area for circumferential cracks with an angle of less than 40° is expected to be zero. If the crack opening area is negligible, the potential flow through the crack should likewise be negligible. Therefore, since 75% of the cracks in the available database have crack angles less than 40°, corresponding to a crack length of 0.24 inch, these cracks would not contribute significantly to any observed leakage. This analysis also validates the prior conclusion that for any crack that would contribute significantly to leakage, the ratio of leakage at SLB condition to that at NOp conditions will always be less than 2.

Based on the lack of occurrence of cracking within the WCGS Unit 1 steam generators, and the structural considerations discussed above, it is expected that at most only a single crack would be present in the H* distance and that crack would be of a limited azimuthal extent (< 40°). It is judged that the presence of a

single crack within the H^* distance would not significantly affect the stiffness of the tube in the hoop direction during all plant conditions and the integrity of the joint would not be compromised.

Concerning primary to secondary leakage, no through wall cracks are expected. In the unlikely occurrence of a throughwall crack in the H^* distance, leakage would be expected to be negligible during all plant conditions due to the small circumferential extent of the crack.

The WCGS Unit 1 plant currently has no repair criteria for degradation found in the steam generators that would allow a tube with any type of indication other than wear to remain in service. Wolf Creek follows the practice as defined in NEI 97-06 Rev. 2, "Steam Generator Program Guidelines," for steam generator inservice inspection, namely plugging based on detection. Plugging of the defective tubes is intended to ensure that tubes remaining in service will meet the integrity performance criteria until the next scheduled tube inspection.

20. Describe the methodology to be employed for performing condition monitoring and operational assessments for the tubesheet inspection zone (for pullout and accident leakage) assuming that SCC and or IGA mechanisms have started to be active.

Response

Condition Monitoring (CM) evaluates the current, as-found, condition of the SG with respect to structural and leakage performance criteria contained in NEI 97-06, Revision 2 (Reference 16). Operational Assessment (OA) is the evaluation of the future state of the SGs to determine if the SGs will meet the structural and leakage performance criteria at the next scheduled inspection. Thus the principal difference between the CM and OA is growth of undetected flaws left in service. For a plug-on-detection scenario, which applies for most forms of corrosion degradation, a key parameter will be the detection limits for the degradation mechanisms of interest in the tubesheet expansion regions as postulated in the RAI, SCC and IGA.

For condition monitoring, flaws in the tubesheet expansion region represent no risk of burst because of the constraint provided by the tubesheet. Therefore, the only concern would be satisfaction of the SLB or accident induced leakage performance criteria. If a single crack is reported in the inspected depth, the crack will be characterized for length and depth (depth may have significant uncertainty) and the leakage from the crack will be calculated based on the crevice model used in the B^* technical justification and compared with the limiting accident analysis primary-to-secondary leakage assumption. If multiple cracks are detected, each crack will be characterized for length and depth, and the total leakage from the cracks will be calculated and compared with the limiting accident analysis primary to secondary leakage assumption.

With regard to the pullout criterion, axial and circumferential cracks will be evaluated to show that pullout resistance is not significantly degraded by the flaws. An axial crack has essentially no impact on the pullout criterion since the entire cross sectional area of the tube and its entire length are still available to resist pullout. Because of the constraint provided by the tubesheet, a throughwall circumferential crack would be constrained to the tensile failure mode. The circumferential crack would be evaluated as to its depth and length to determine the load carrying capability of the tube. As a first estimate, it would be assumed that the entire crack length is 100% throughwall, the percent degraded area (PDA) of the tube

calculated and the results compared to the acceptable PDA for tensile failure under accident loading conditions. A very long and deep crack (approximately 75 PDA) is required to exceed the tensile load carrying capability of the tube under accident without benefit of any residual restraining forces due to the expansion process. The measured crack length is inherently conservative due to lead-in, lead-out of the probe.

For Operational Assessment, since any observed cracking within the inspected region of the tubesheet expansion region would be plugged on detection, the only issue influencing the evaluation would be the detection limit of cracks within this region. If no change in cycle length or operating conditions is anticipated, the incidence (as well as the characteristic) of detected cracking can be assumed to be the same as the prior cycle.

As an alternative, the EPRI Tube Integrity Assessment Guidelines (Reference 17) provide a basis for conservatively determining the size of an undetected crack in the event insufficient data are available to determine the POD for cracks in this region. A conservative estimate of growth rate can be developed from the data available for the mill annealed Alloy 600 tubing in the original SGs at Callaway (See response to RAI# 19). Using this data is conservative since it is for Alloy 600MA tubing in which the incidence and progression of SCC is more rapid than in Alloy 600TT tubes as utilized in the Wolf Creek SGs.

21. Enclosure 1: The development of the B distances assumes that crack leakage resistance is not significant relative to the tube-to-tubesheet joint resistance. Discuss the conservatism of the B* distances given the assumption that crack leakage resistance is the dominant resistance to leakage under normal operating conditions. To the extent this discussion relies on assumptions about contact pressure between the tube and tubesheet local to the crack, justify assumptions relative to the influence of the crack on local contact pressure.*

Response

Below an H* distance of 9 inches, crack leakage resistance is the dominant leakage resistance under normal operating conditions and SLB conditions, but only for very short cracks (< 0.250 inch). See Figure 18. Leakage during all plant conditions for cracks of this size is predicted to be negligible. For larger cracks, crevice leakage resistance is the dominant resistance to leakage under both normal operating and SLB conditions. Cracks > 0.25 inches but < 0.5 inches in azimuthal extent only provide a small amount of additional resistance to leakage during all plant conditions. The additional leakage resistance would only lessen the calculated B* distances. Cracks that are > 0.5 inch in azimuthal extent result in no significant increase in leakage resistance during all plant conditions. Above an H* distance of 9 inches, there is no significant effect due to crack leakage resistance even for very short cracks. See Figure 19. Based on the above, it is judged that crack leakage resistance has a negligible impact on the B* distances calculated for WCGS Unit 1.

Moreover, cracks of < 0.5 inches in azimuthal extent are judged to have a negligible influence on local contact pressure between the tube and the tubesheet as the stiffness of the tube should be largely unaffected. For another type of expansion (mechanical roll), the (end) effect on radial contact pressure was limited to a distance of []^{a,c,e} for a tube that was postulated to be completely severed in the tubesheet. It is expected, based on the analysis results, that in the event of a full guillotine sever in the

tube the stresses in the region local to the sever would redistribute such that the end effect would be equal to []^{a,c,e} or less (Reference 14).

a,c,e



Figure 18: Plot of Leak Resistance vs. Crack Half-Length, at a Typical Peripheral Location, 9 inches below the TTS Assuming that the Crack Elevation is Considered Below the H^* Depth. $DP = 1.00$; Crevice Pressure Modifications are Included. Contact Pressure is Calculated Using the B^*/H^* Theory of Elasticity Model and the Loss Coefficients are Taken from the Model F Data Set



Figure 19: Plot of Leak Resistance vs. Crack Half-Length, at a Typical Peripheral Location, 9 Inches Below the TTS Assuming that the Crack Elevation is Considered Above the H* Depth. DP = 1.00; Crevice Pressure Modifications are Included. Contact Pressure is Calculated Using the B*/H* Theory of Elasticity Model and the Loss Coefficients are Taken from the Model F Data Set

22. *Describe the methodology for performing condition monitoring and operational assessments for accident induced leakage stemming from locations below the specified tubesheet inspection depths.*

Response

If leakage from below the specified inspection distance is observed prior to the postulated accident and is within the specified normal operating condition leakage limit (150 gpd), the analysis shows that the accident induced leakage will not exceed the accident induced leakage limits. The Accident induced leakage will be bounded by a factor of no greater than 2 times the Normal Operating condition leakage limit. If no other sources of leakages are identified in the SG, the observed NOP leakage will be multiplied by 2 to determine the accident induced leakage, and the result will be compared to the leakage limit assumed in the Safety Analysis for the plant for the limiting accident, 1gpm.

If zero leakage is observed prior to a postulated accident, it is judged that zero leakage will occur during a postulated accident. It is judged that the likelihood of ligament tearing of circumferential cracks and/or axial cracks resulting from an accident pressure increase is small, since at most, only 9% of the cross-sectional area of the tube is needed to maintain tube integrity. For example, for a circumferential crack, the difference in the applied force as a result of normal operating and accident condition loadings is very small (~ 50 lbs). Therefore, the potential for ligament tearing is considered to be a secondary effect of negligible probability.

23. *By letter dated March 28, 2006, you provided revisions to your proposed technical specifications (TS) in accordance with TSTF-449, Rev. 4, to include the following additional sentence into TS 5.5.9 c.1:*

"All tubes with degradation identified in the portion of the tube within the region from the top of the hot leg tubesheet to 17 inches below the top of the tubesheet shall be removed from service."

Describe your plans for revising these words to reflect the February 21, 2006 license amendment and for submitting revisions to this amendment.

Response - WOLF CREEK RESPONSE

The response to this question is provided in Attachment I.

24. *Discuss your plans to revise TS 5.6.10 to include reporting requirements applicable to the implementation of the tubesheet inspection and alternate repair criteria. For example:*

- * *A breakout of indications detected within the tubesheet inspection depths with respect to their location, orientation, and measured size. (The only difference here relative to proposed changes associated with Technical Specification Task Force (TSTF) 449, Revision 4, is that the indications in the tubesheet region would be listed separately from those elsewhere.)*

- * *The operational primary to secondary leakage rate observed in each steam generator during the cycle preceding the inspection which is the subject of the report, and (2) the calculated accident leakage rate for each steam generator from the portion of tubing below the tubesheet inspection depths for the most limiting accident. If the calculated accident leakage rate for any steam generator is less than 2 times the total observed operational primary to secondary leakage rate, the 12-month report should describe how it was determined.*

Response - WOLF CREEK RESPONSE

The response to this question is provided in Attachment I.

25. *Enclosure 1, Section 7.1.3, page 46 of 127: The tubesheet bow analysis takes credit for resistance against bow provided by the divider plate. Cracks in the welds connecting the tubesheet and divider plate have been found by inspection at certain foreign steam generators. Describe what actions you are taking to ensure that the divider plates can perform their function, including providing the assumed resistance against tubesheet bow.*

Response

Indications of cracks in the divider plates have been reported in French steam generators located at the Chinon, Saint-Laurent, Dampierre and Gravelines nuclear power stations. The cracks were observed on the hot leg side of the divider plate in the stub runner divider plate weld, stub runner base metal and also at or in the divider plate itself. Figure 20 is a sketch of the region where cracking has been observed to occur.

The divider plate has typically been accounted for in B* and H* analyses via a divider plate factor, which is the ratio of the maximum vertical tubesheet displacements with an intact divider plate compared to the maximum vertical displacements of a tubesheet with no divider plate present. The factor is based on the ASME Code Stress Report provided for the SGs, which considered both to conservatively calculate stresses in the tubesheet and stresses in the components attached to the tubesheet. Based on the original ASME Code stress analysis, the ratio of the maximum tubesheet displacement with and without the benefit of the divider plate is []^{a,c,e} which means that the maximum vertical displacement of the tubesheet with an intact divider plate is []^{a,c,e} less than the maximum vertical displacement of a tubesheet without a divider plate. This value []^{a,c,e} was used for the divider plate factor in the B* and H* analyses prior to 2007. A value of 1.00 for the divider plate factor is used in the H* and B* analyses to evaluate the condition where the divider plate does not restrain the vertical tubesheet displacements of the tubesheet.

The divider plate factor from the ASME stress report was determined by comparing the results of finite element models that included a divider plate with the nominal material properties and dimensions to a divider plate with an artificially low stiffness (e.g. Young's Modulus = 10 psi). The finite element models utilized for the code stress report to determine the divider plate effect were overly conservative because they did not account for features in the lower steam generator assembly that act to increase the resistance of the tubesheet to vertical deflections. For example, in the early analysis models used to calculate tubesheet displacements, the tubelane and the channel head to divider plate weld were not modeled. Research by Terakawa (Reference 15) indicates that the presence of the tube material within

the tubesheet acts to stiffen the tubesheet with respect to bending and vertical deflection. A more detailed finite element model than that used in the original stress analysis shows that the impact of a non-degraded divider plate on tubesheet deflection is significantly greater and that the appropriate value to use for the divider plate factor in H^* and B^* analyses is []^{a,c,e} (Reference 10), that is, the tubesheet deflection with an intact divider plate is significantly less than originally estimated.

The effect of a reduced divider plate factor with a non-degraded divider plate will decrease the value of H^* and B^* since the tubesheet hole dilation above the neutral plane of the TS is significantly less with smaller tubesheet displacement. This result would also be true for the type of cracks found in the French units, i.e. small depths with apparent low growth rates. Therefore, it is concluded that the current analysis for H^* and B^* is inherently conservative due to the overestimate of the tubesheet deflection.

The B^*/H^* results presented in the responses to these RAI include a non-functional divider plate (DP = 1.00) except where noted as otherwise. Note that in this context the term “non-functional” applies only to the divider plates ability to restrain the vertical deflections of the tubesheet.

Because the original tubesheet analysis is inherently conservative, and because the calculations based on the revised structural model and the revised tubesheet crevice pressure model show that the extreme case of the divider plate absent have only a small effect on the values of H^* and B^* , regular inspection of the tubesheet primary side using the current visual inspection techniques (bowl camera) is adequate to assure continued function of the divider plate. Evaluation of the current divider plate degradation indicates that the progression of degradation is small, and that very significant divider plate degradation is required before the function of the divider plate relative to the deflection of the tubesheet would be degraded.

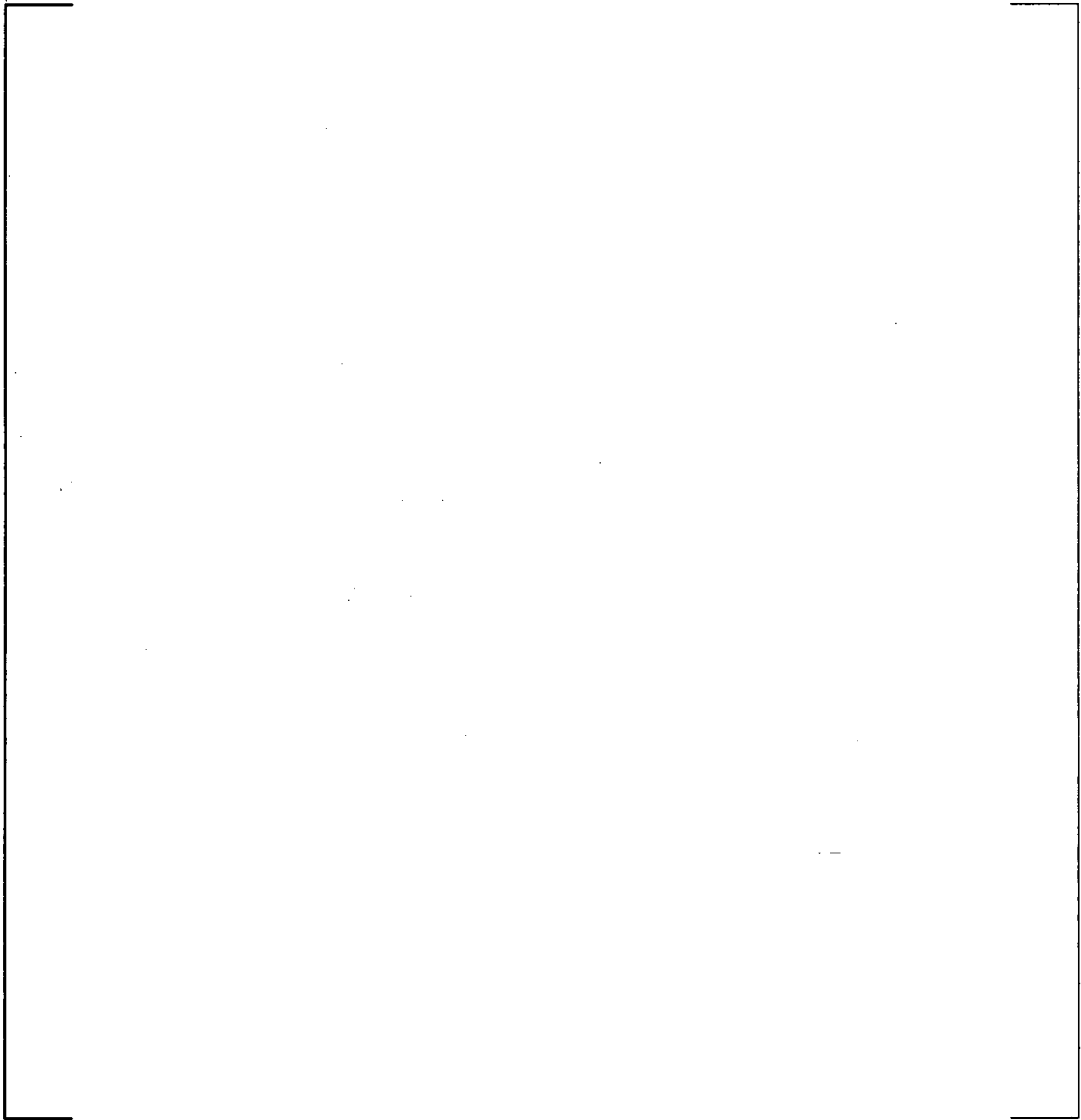


Figure 20: Sketch of Divider Plate, Channel Head and Tubesheet with Potential Cracking Areas Highlighted

26. *An observation (in that no response is needed) - On page 24 of 127 of Enclosure 1 to the referenced submittal, an item 3 should be added as follows: Calculated primary-to-secondary side leak rate during postulated events should [read]:*

1) ..

2) ...

3) *not exceed 1 gallon per minute (gpm) per steam generator (SG)*

Response

No response is needed.

References:

1. NCE-88-271, "Assessment of Tube-to-Tubesheet Joint Manufacturing Processes for Sizewell B Steam Generators Using Alloy 690 Tubing," November 1988.
2. LTR-SGDA-03-129, "Transmittal of Responses to NRC RAIs on Partial-Length RPC Inspection of the Tubesheet Region of the Callaway Plant Steam Generators to AmerenUE Callaway (Class 2 Document)," 6/2/03.
3. WCAP-15932-P, Rev. 1, "Improved Justification of Partial-Length RPC Inspection of the Tube Joints of Model F Steam Generators of Ameren-UE Callaway Plant," May 2003.
4. Goodier, J., and Schoessow, G., "The Holding Power and Hydraulic Tightness of Expanded Tube Joints: Analysis of Stress and Deformation," Transactions of the ASME, New York, New York, USA (July 1943).
5. Formulas of Stress and Strain, Fifth Edition, Roark, R., and Young, W., McGraw-Hill Book Company, New York, New York, USA (1975).
6. CN-SGDA-02-127, "Evaluation of Tube/Tubesheet Contact Pressures for Wolf Creek, Seabrook, and Millstone 3 Model F Steam Generators," Westinghouse Electric, Madison, PA, USA (August 2002).
7. LTR-CDME-07-74, "Supporting Analysis for Wolf Creek H*/B* RAI Responses," April 2007.
8. TH-98-37, "Vogle/Yonggwang Tubesheet Crevice Leakage," 10/3/98.
9. "Stress Analysis of Thick Perforated Plates," PhD Thesis by T. Slot, Technomic Publishing Co., Westport, CN, 1972.
10. LTR-SGDA-07-4, "Letter Summary of Changes to B* and H* Analysis due to New Crevice Pressure and Divider Plate Data," January 18, 2007.
11. ASME Boiler and Pressure Vessel Code Section III, "Rules for Construction of Nuclear Power Plant Components," 1989 Edition, The American Society of Mechanical Engineers, New York, NY.
12. "Improved Justification of Partial Length RPC Inspection of Tube Joints of Model F Steam Generators of Ameren-UE Callaway Plant," WCAP-15932, Revision 1, May 2003.
13. EPRI Tube Integrity Tools Theory Manual, Final Report, May 2006.
14. WCAP-15004, "F* Tube Plugging Criterion for Tubes with Degradation in the Tubesheet Region of the Comanche Peak Unit 1 Steam Generators," December 1997.

15. Terakowa, T. Imai, A., Yagi, Kazushige, Fukada, Y., Okada, K., "Stiffening Effects of Tubes in Heat Exchanger Tubesheet," Journal of Pressure Vessel Technology Transactions, ASME Vol. 106, No. 3, August 1984.
16. NEI 97-06, Revision 2.
17. EPRI 1012987, "Tube Integrity Assessment Guidelines, Revision 2," July 2006.
18. WNEP-8448, "Hydraulic Expansion of Steam Generator Tubes Into Tubesheet," December 1983.
19. WCAP-16670-P, "Steam Generator Alternate Repair Criteria for Tube Portion Within the Tubesheet at Comanche Peak Unit 2," November 2006.
20. STD-DP-1997-8015, Rev. 0, "Data Package for Leak Testing of Vogtle Unit 1 Steam Generator Tube to Tubesheet Joint Per STD-TP-1997-7951 Rev. 1," 6/13/97.
21. LTR-SGDA-06-108, "Data and Analysis Methodology in Support of Axial Ligament Tearing Model," June 29, 2006.

APPENDIX A

LTR-SGDA-07-4

Letter Summary of Changes to B* and H* Analyses
Due to New Crevice Pressure and Divider Plate Data,

January 17, 2007



To: H.O. Lagally

Date: January 17, 2007

cc: P.R. Nelson

G.W. Whiteman

J.G. Thakkar

E. P. Morgan

B.A. Bell

W.K. Cullen

N.R. Brown

From: C.D. Cassino

Your ref:

Ext: 724 722-5134

Our ref: LTR-SGDA-07-4

Fax: 724 722-5889

Subject: **Letter Summary of Changes to B* and H* Analysis due to New Crevice Pressure and Divider Plate Data**

The technical basis for H* and B* as documented in the Alternate Repair Criteria (ARC) WCAPs and Calc Notes (see Reference 2 for an example) is based, in part, on of the fundamental assumption that leakage through a postulated crack below H* flashes to steam in the crevice. This establishes the pressure in the crevice as the saturation pressure. Recent test data show that leakage through a crack below H* does not flash to steam and remains a single-phase fluid; therefore, the original assumption is not justified and changes must be made to the B* and H* analysis inputs to reflect the new test results.

The purpose of the test was to determine the pressure in the crevice between the tube and the tubesheet. The tests show that there is a distribution of pressure in the tubesheet crevice that is typically much greater than the secondary side pressure under NOP (P ~ 800 psi) or SLB (P ~ 0 psi) conditions. The results showed that the fluid in the crevice remained single phase to very near the end of the []^{a,c,e} Therefore, the crevice pressure is higher than originally assumed in the H*/B* analyses. An increased pressure in the crevice will result in:

1. Reduced driving head on any fluid in the crevice.
2. Increased resistance to flow due to viscous effects.
3. Reduction of the tube expansion component of the contact pressure analysis.
4. Reduction of the tube expansion component of the leakage resistance analysis.

Incorporating the recent crevice pressure test data does not significantly change the results of the B* and H* analysis.

Further, the issue of divider plate degradation effects on the H*/B* analyses has been raised. This issue has not been directly addressed in the technical justification for H* and B*, but has been preliminarily studied. The bounding value for H* and B* within the tubesheet is estimated at approximately 12 inches in a steam generator with a fully degraded divider plate. The range of inspection depths for a true B* approach, or a bounding B* depth approach, still provide significant margin for a permanent 17 inch B* application or inspection depths approaching the neutral axis of the tubesheet.

Note that the flaw in the test specimens discussed in this document was specifically designed to eliminate issues with crack geometry. It is possible to maintain a large pressure drop across the tube wall in some crack geometries. A larger pressure drop across the tube wall would decrease the pressure in the crevice.

If there are any questions regarding the contents of this letter please contact either Chris Cassino or Jivan Thakkar.

Author:

C.D. Cassino

Chemistry, Diagnostics and Materials Engineering

Reviewer:

J. G. Thakkar

Steam Generator Design and Analysis

References

1. STD-MC-06-11, R.J. Jacko, Profile Measurements during Tube-to-Tubesheet Leakage Tests of Hydraulically Expanded Steam Generator Tubing", June 2006. (proprietary)
2. LTR-CDME-05-32-P, Rev. 2, G.W. Whiteman, "Limited Inspection of the Steam Generator Tube Portion within the Tubesheet at Byron 2 & Braidwood 2", August 2005. (proprietary)
3. <http://ewr.cee.vt.edu/environmental/teach/smprimer/outlier/outlier.html>, 12/07/2006, 01:14:06 PM EST.
4. M.R. Chernick, "A Note on the Robustness of Dixon's Ratio Test in Small Samples", *American Statistician*, Vol. 36, No. 2 (May, 1982), p. 140.
5. W.B. Middlebrooks, D.L. Harrod, R.E. Gold, "Residual Stresses Associated with the Hydraulic Expansion of Steam Generator Tubing into Tubesheets," *Nuclear Engineering and Design* 143 (1993) 159-169 North-Holland.
6. LTR-SGDA-06-156, "Potential Effect of Cracks in Westinghouse Steam Generator Divider Plates Considering EDF Cracking History," August 28, 2006.
7. LTR-SGDA-06-157, C.D. Cassino, "B*/H* Bounding Cracked Divider Plate Analysis," 8/31/06.
8. CN-SGDA-07-6, C.D. Cassino, "Finite Element Analysis of a Degraded Alloy 600 Stub Runner to Divider Plate weld in Non-Center Stayed Steam Generators ," January 2007.
9. Terakawa, T., Imai, A., Yagi, Kazushige, Fukada, Y., Okada, K., "Stiffening Effects of Tubes in Heat Exchanger Tube Sheet", *Journal of Pressure Vessel Technology Transactions, ASME* Vol. 106, No.3, August 1984.
10. LTR-SGDA-06-160, J.G. Thakkar, "Letter of Transmittal for Millstone Unit 3 True B* Microsoft Excel Workbooks for WCAP-16656-P," 09/19/2006.
11. LTR-SGDA-07-3, B.A. Bell, "Summary of H* and B* Analysis Crevice Pressure Changes and Results," 01/16/2007.
12. TP-SGDA-03-2, Rev.1, D.P. Popovich, "Model D5 Tube-to-Tubesheet Joint Determination of Leakage Resistance for H-Star Program for Comanche Peak 2, Catawba 2, Byron 2 and Braidwood 2," 09/17/2003.

1.0 Discussion of Crevice Pressure Test Results

The tests documented in Reference 1 were performed to determine the pressure distribution in the crevice of a hydraulically expanded tubesheet region with a postulated through wall flaw near the bottom of the expansion. Two test specimens were prepared that simulated the normal operating (NOP) and main steam line break (SLB) conditions of an Alloy 600TT tube within the tubesheet. The flaw in the test specimens was [

in order to remove concerns about crack geometry from the leakage results [12]. Note that in a real crack in a tube it is possible to maintain a large pressure drop across the tube wall. Therefore, the results discussed in the following sections should be considered as conservative estimates. Both of the test specimens (Figure 1) have the same geometry and were pre-treated (i.e. hydraulically expanded into the collar, heat relieved, etc.) similarly. The fluid used in the studies was simulated primary water under simulated steam generator conditions (i.e. temperature and pressure). The data from the NOP and SLB tests from both specimens [1], taken after the pressure in the crevice reached steady state conditions, are shown in Table 1 and Table 2 below.

Table 1: Crevice Pressure Specimen Data from Steady State NOP Conditions

a,c,e

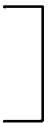
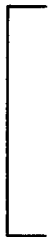


Table 2: Crevice Pressure Specimen Data from Steady State SLB Conditions

a,c,e



a,c,e

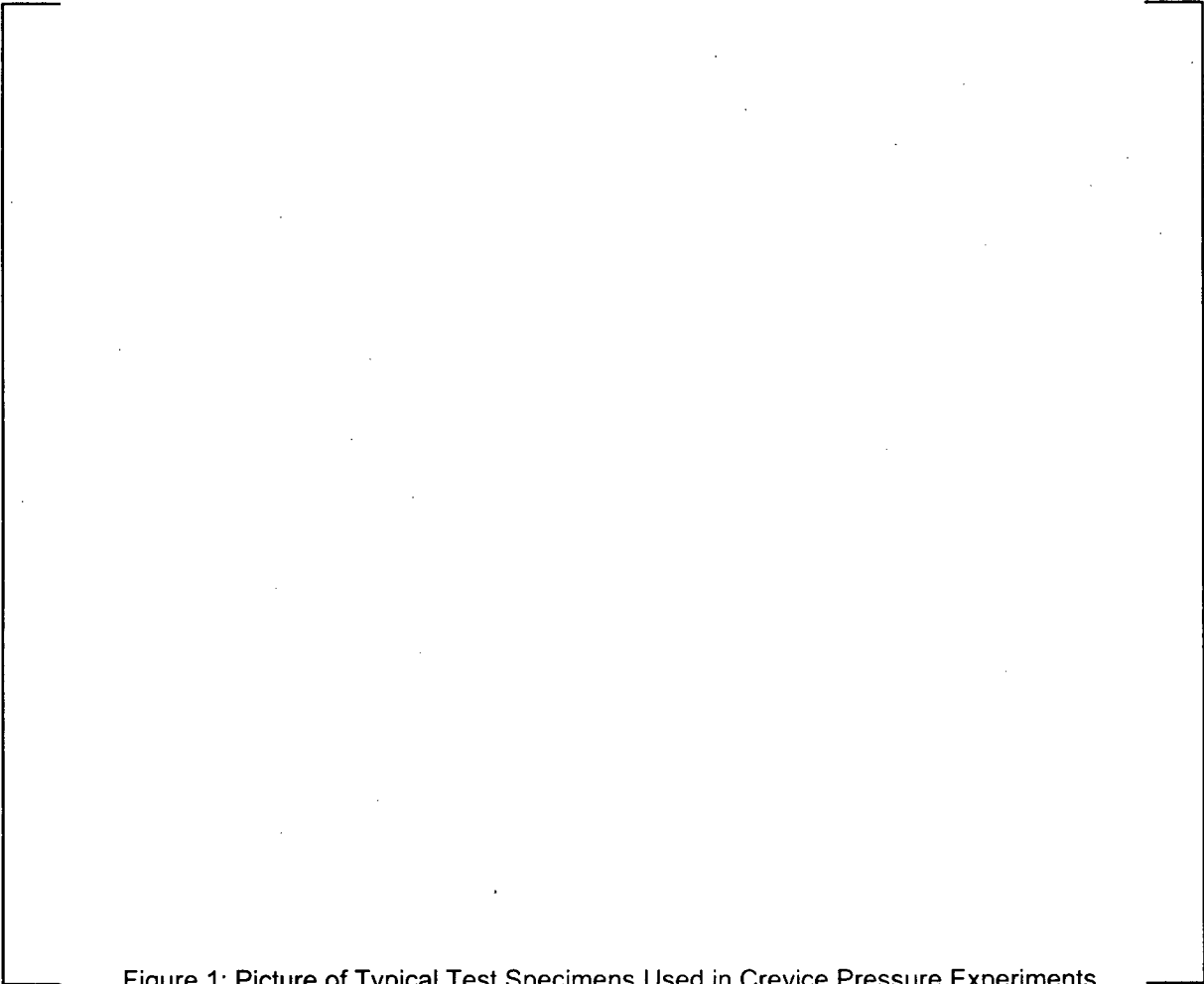


Figure 1: Picture of Typical Test Specimens Used in Crevice Pressure Experiments.

The pressure taps shown in Figure 1 begin at [

] ^{a,c,e} Figure 2 and Figure 3 are plots of the combined test results for both specimens during the simulated normal operating (NOP) condition and the simulated steam line break (SLB) condition. The results in both Figure 2 and Figure 3 are normalized to facilitate comparisons to a tubesheet. The depth ratio in each plot is the distance to the pressure tap divided by the total expansion distance of the specimen. (The expansion length is less than the sample length.) The crevice pressure ratio is the pressure measured in the crevice at the elevation of each pressure tap divided by the primary side pressure.

a,c,e



Figure 2: Plot of Crevice Pressure Ratio as a Function of Depth Ratio into the Test Specimen for Simulated NOP conditions.

a,c,e



Figure 3: Plot of Crevice Pressure Ratio as a Function of Depth Ratio into the Test Specimen for Simulated SLB conditions.

An important conclusion from these tests is apparent from Figure 2 and Figure 3: The pressure in the crevice under NOP and SLB is high enough to keep the fluid single phase in the entire crevice up to nearly the top of the test specimen. The prior H^*/B^* analyses had assumed that the full secondary side pressure during each condition was present in the crevice due to the assumption that the liquid would flash to steam immediately outside the postulated flaw.

2.0 Conclusions relative to H^* and B^* Analysis

The tests [1] show [that the distribution of pressure in the tubesheet crevice that is typically much greater than the secondary side pressure under NOP ($P \sim 800$ psi) or SLB ($P \sim 0$ psi) conditions. The fluid in the crevice remains single phase and the pressure drop and reduction in viscosity that comes from the primary water flashing to steam does not occur until near the top of the simulated tubesheet. Also, because the crevice pressure is higher than the secondary side pressure, the large drop in pressure across the tube wall that acted to increase the contact pressure between the tube and the tubesheet in the current analysis method has been reduced. The sum of the conclusions suggests that the following changes should be made in the H^*/B^* analysis:

1. The driving head on the leaked fluid has been reduced.
2. The resistance to flow from viscous effects has increased.
3. The tube expansion component of the contact pressure analysis has been reduced.
4. The tube expansion component of the leakage resistance analysis has been reduced.

Points 1 and 2 mean that the prior assumptions on leak rate through a crack in a tube were overly conservative. Points 3 and 4 mean that the prior assumptions about resistance against leakage and structural issues were non-conservative. In the context of this discussion the term conservative is taken to mean that the input assumptions in the analysis maximize the potential leakage through a postulated crack into the tubesheet crevice during accident conditions while penalizing the tube retention capability of the tube/tubesheet interface.

The contact pressure between the tube wall and the tubesheet hole is calculated in the H^* and B^* analysis for two reasons:

1. It determines the loss coefficient for the leakage in the crevice.
2. It determines the engagement length necessary to equilibrate the far field axial load on the tube.

The components that contribute to the contact pressure between the tube material and the tubesheet crevice are:

- The radial tube expansion due to thermal growth of the tube material and the tubesheet crevice,
- Pressure differential across the tube wall,

- Distortion of the tubesheet crevice due to the primary to secondary pressure differential and any
- Residual effects from the hydraulic expansion process. This is the smallest contribution to the contact pressure [5].

Of these, only the contribution of the contact pressure due to the pressure differential across the tube wall is affected by the increase in crevice pressure. The contribution of the thermal growth in each material will not be affected by an increase in the crevice pressure. Similarly, the tubesheet distortion and residual expansion effects are not affected by the increased crevice pressure either.

The unrestrained radial expansion of a tube OD due to a pressure differential across the tube wall is

$$\Delta R_{to}^{pr} = \frac{P_i c}{E_t} \left[\frac{(2 - \nu) b^2}{c^2 - b^2} \right] - \frac{P_o c}{E_t} \left[\frac{(1 - 2\nu) c^2 + (1 + \nu) b^2}{c^2 - b^2} \right],$$

Where: P_i = Internal primary side pressure, P_{Pri} psi
 P_o = External secondary side pressure, $P_{Crevice}$ psi
 b = Inside radius of tube
 c = Outside radius of tube
 E_t = Modulus of Elasticity of tube, psi
 ν = Poisson's Ratio of the material.

In the original analysis, P_o was assumed to be equal to the secondary side pressure. If the value of P_o is increased, the value will ΔR_{to}^{pr} decrease. For example, if during NOP the primary side pressure is 2235 psi and the secondary side pressure is 800 psi the pressure differential between the two is 1435 psi. If the crevice pressure is greater than the secondary side pressure, say 1350 psi, the pressure differential across the tube wall decreases to [

] ^{a,c,e}

The test results show that the crevice pressures decreases along the depth of the tubesheet crevice with greater distance from the flaw. The test results also show that at the lower elevations, there is very little pressure differential across the tube wall while at the higher elevations there is a large pressure differential across the tube wall. There are several models that could apply this data to the B* and H* analyses:

[

] ^{a,c,e}

The pressure distribution profiles in the tubesheet crevice are shown in Figure 4 and Figure 5 below, for both accident and normal operating conditions.



Figure 4: Plot of Crevice Pressure Model Comparisons using average test data results for the normal operating condition.



Figure 5: Plot of Crevice Pressure Model Comparisons using average test data results for the SLB accident condition.

For conservatism and simplicity, the analysis utilizes a limiting crevice pressure ratio to define the pressure in the tubesheet crevice during operating and accident conditions. The limiting value of the crevice pressure should be taken such that it yields a conservative (lower) estimate of the contact pressure and the corresponding B^* and H^* depths. The trend of the curves in Figures 2 and 3 is that the crevice pressure [

]a.c.e

A commonly used statistical tool to determine outliers in a limited population of data is the Dixon Ratio test. The following text is adapted from the tutorial on the detection and accommodation of outliers from the web library of Virginia Polytechnic Institute and State University department of Civil and Environmental Engineering [3]. Dixon's test is generally used for detecting a small number of outliers. This test can be used when the sample size is between 3 and 25 observations [4], but is typically employed whenever a sample set is less than an ideal population to apply standard statistical tools. The data is ranked in ascending order and then sorted on the sample size. The τ statistic for the highest value or lowest value is computed. Note that eliminating the outliers in the distributions shown in Figures 2 and 3 will not affect the normality of the distribution. Also note that the skewness of the distributions shown in Figures 2 and 3 is less than ± 0.5 so it is appropriate to assume that both the NOP and SLB data are appropriately normal and that the Dixon's Ratio test can apply. The chart below gives a list of how to calculate the appropriate Dixon Ratio values.

Observations	Highest value suspect	Lowest value suspect
3 to 7	$\tau = \frac{X_n - X_{n-1}}{X_n - X_1}$	$\tau = \frac{X_2 - X_1}{X_n - X_1}$
8 to 10	$\tau = \frac{X_n - X_{n-1}}{X_n - X_2}$	$\tau = \frac{X_2 - X_1}{X_{n-1} - X_1}$
11 to 13	$\tau = \frac{X_n - X_{n-2}}{X_n - X_2}$	$\tau = \frac{X_3 - X_1}{X_{n-1} - X_1}$
14 to 20-30	$\tau = \frac{X_n - X_{n-2}}{X_n - X_3}$	$\tau = \frac{X_3 - X_1}{X_{n-2} - X_1}$

The τ statistic is compared to a critical value at a chosen value of α . If the τ statistic is less than the critical value, the null hypothesis is not rejected, and the conclusion is that no outliers are present. If the τ statistic is greater than the critical value, the null hypothesis is rejected, and the conclusion is that the most extreme value is an outlier. To check for other outliers, the Dixon test can be repeated, however, the power of this test decreases as the number of repetitions increases.

As an example, calculating the Dixon Ratio value for the NOP condition in Model 1 yields a value of [

] ^{a,c,e} The data used to calculate the Dixon ratio for each model is shown below. (These data are derived from Figures 2 and 3.)

Table 3: Dixon Ratio test input and results for NOP condition.

	a,c,e
[]

Table 4: Dixon Ratio test input and results for SLB condition.

	a,c,e
[]

The effects of the results of the tests performed to determine the crevice pressure conditions on H* and B* are evaluated in section 4.0.

3.0 The Effect of the Divider Plate Factor on B* and H* Analysis

Indications of cracks in the divider plates have been reported in several steam generators located in France. These indications have been observed in steam generators located at the Chinon, Saint-Laurent, Dampierre and Gravelines nuclear power stations. The cracks were observed on the hot leg side of the divider plate in the stub runner divider plate weld, stub runner base metal and also at or in the divider plate itself. See Figure 3 for a sketch of the region where cracking has been observed to occur.

a,c,e



Figure 6: Sketch of Divider Plate, Channel Head and Tubesheet with potential cracking areas highlighted.

The network of cracks has been reported to extend along most of the divider plate (~6 feet) and have also been reported to be relatively shallow with depth, typically less than 2 mm (~75 mils deep).

The French utilities inspected this location to determine if any indications of cracking could be found during a visual inspection because these steam generators used an Alloy 600 material in the divider plate to stub runner weld. During the initial visual inspection it was reported that indications of cracks were observed but that they appeared to be shallow in depth. Various other methods were used in subsequent refueling outages to determine the extent of cracking and to determine the crack growth rate. Available information indicates that these inspections have been performed since 1993 using a combination of liquid penetrant examination (PT) and visual examination (VT) methods with indications of cracking observed in some of these plants. Through the winter of 2005, a total of thirty five inspections using VT and PT were performed in the French 900 megawatt (MW) and 1300 MW units with indications of cracking being found in at least four of the plants as noted above.

Primary water stress corrosion cracking (PWSCC) is a know mechanism of cracking in Alloy 600 and it is likely this is the primary contributor to cracking at this location.

However, other potential contributors to cracking have been reported to be defects in the weld or base material, along with deformations associated with loose part impingement and these may be contributing factors.

The maximum depth of the majority of the cracks observed in the French units has been reported to be about 2 mm (~75 mils). The maximum crack depth indication that has been observed is 7 mm (~0.28 inch) however this indication is the likely result of loose part damage on the hot leg side of the divider plate in the affected generator. Various inspection methods (VT, PT, and then UT) have been used in plants with indications of divider plate cracking. It has been reported that consecutive inspections using identical methods have not been performed to date; therefore, it is not possible to develop an accurate growth rate from the French inspection data. From the available information it can be inferred that the cycle-to-cycle growth rate of the cracks is small based on the following: The difficulty in obtaining an accurate measure of the depth of the crack due to the shallowness of the crack (smaller cracks are harder to detect than larger cracks), the continued reports of finding only shallow depth cracks, and the relatively long period of time that these cracks have been known to exist.

The majority of the cracks included by the French experience are small with relatively small cycle-to-cycle growth rates, therefore, the effect on the divider plate function is also expected to be small. It would be expected that cracks of the size reported would not affect the general displacement response of the tubesheet since only a very small change in divider plate stiffness would be expected. In addition, it would not be expected that cracks of the size reported would rapidly grow due to mechanically induced loadings resulting from normal/upset events or during a faulted event. However, there may be a potential for long term growth of these cracks which could eventually affect tubesheet displacements and result in an increased rate of crack propagation.

Westinghouse has performed an analysis to determine the effect of these types of cracks in the divider plate on longer term operation. The scope of work includes determining the consequences of relatively large (but not totally through-wall) cracks in the divider plate. Through-wall cracks are not likely to rapidly occur based on the French experience. The analysis will consider the effect of increased tubesheet displacements and the resulting stress near the crack tip which may propagate the crack due to mechanical methods.

Tubesheet displacements can directly affect multiple regions in the SG that include such areas as:

- a. Tubesheet stress
- b. Secondary side shell stress
- c. Channel head stress
- d. Tube stress
- e. Plug retention/acceptability issues.

The divider plate has typically been accounted for in B* and H* analyses via a divider plate factor, which is the ratio of the maximum vertical tubesheet displacements with an intact divider plate compared to the maximum vertical displacements of a tubesheet with

no divider plate present. The factor is based on the ASME stress report provided for the SGs, which considered both to conservatively calculate stresses in the tubesheet and in the components attached to the tubesheet. The ratio of the maximum tubesheet displacement with and without the benefit of the divider plate is 0.76, which means that the maximum vertical displacement of the tubesheet with an intact divider plate is 24% less than the maximum vertical displacement of a tubesheet without a divider plate based on the ASME Code Stress Report for the SGs. This value (0.76) is used for the divider plate factor in the B^* and H^* analyses prior to 2007. A value of 1.00 for the divider plate factor is used in the H^* and B^* analyses to evaluate the condition where the divider plate does not restrain the vertical tubesheet displacements of the tubesheet.

The divider plate factor from the ASME stress report was determined by comparing the results of finite element models that included a divider plate with the nominal material properties and dimensions to a divider plate with an artificially low stiffness (e.g. Young's Modulus = 10 psi). The finite element models utilized for the code stress report to determine the divider plate effect were overly conservative because they did not account for features in the lower steam generator region that act to increase the resistance of the tubesheet to vertical deflections. For example, in the early analysis models used to calculate tubesheet displacements, the tubelane and the channel head to divider plate weld were not modeled. Research by Terakawa [9] suggests that the presence of the tube material within the tubesheet acts to stiffen the tubesheet with respect to bending and vertical deflection. A more detailed finite element model than that used in the original stress analysis shows that the impact of a non-degraded divider plate on tubesheet deflection is significantly greater and that the appropriate value to use for the divider plate factor in H^* and B^* analyses is 0.399 [8], that is, the tubesheet deflection with an intact divider plate is significantly less than originally estimated.

The effect of a reduced divider plate factor with a non-degraded divider plate will decrease the value of H^* and B^* since the tubesheet hole dilation is significantly less with smaller tubesheet displacement. This result would also be true for the type of cracks found in the French units, i.e. small depths with apparent low growth rates. Therefore, it is concluded that the current analysis for H^* and B^* is inherently conservative due to the overestimate of the tubesheet deflection.

To evaluate the effect of a degraded divider plate, a bounding analysis was performed which assumed that the divider plate provides no restraint against tubesheet deflection (i.e. $DP = 1.00$). The structural model used in this bounding analysis was the improved finite element model. The bounding value for H^* and B^* using the previous model assumptions (with the secondary side pressure in the crevice) was estimated to be 12 inches [7]. For inspection depths of greater than 12 inches, the absence of the divider plate has no significant effect. A detailed analysis is required to establish the true B^* distance assuming no restraint provided by the divider plate, or factoring in updated information on the growth of divider plate degradation.

Evaluation of divider plate degradation is continuing under EPRI sponsorship. The effects of long term operation with postulated larger cracks in the divider plate must be evaluated to determine if the cracks could grow to a point where either rapid crack growth could occur during operation of the SG or if increased tubesheet displacements could affect other aspects of the steam generator, such as tubesheet stress, secondary side shell stress, channel head stress, tube stress, plug retention/acceptability issues and the ARCs [6].

The following conclusions are reached based on the current evaluation of divider plate degradation:

1. The original divider plate factor from the ASME Code stress report, the ratio of the maximum tubesheet displacement assuming a fully effective divider plate to that assuming no contribution from the divider plate, is 0.76.
2. Based on a more detailed finite element model of the tubesheet/divider plate assembly, the revised divider plate factor is 0.399.
3. The preliminary conservative estimate of H^* and B^* assuming no structural contribution from the divider plate is bounded by 12 inches from the top of the tubesheet.
4. The presence or absence of the divider plate does not impact a 17" inspection depth, since sufficient margin exists between the estimated bounding value (12 inches) and the 17 inch inspection depth. The structural model used for this assessment is the refined finite element model of the tubesheet/divider plate assembly.
5. The exact value of the "true" B^* requires additional analysis but is not expected to be greater than 12 inches.

4.0 Results from Implementing Changes in H* and B* Analysis

Table 5 below summarizes the limiting crevice pressure ratios from the three different models using 1) the mean of the entire data set, 2) the median of the entire data set, 3) a skewed mean and median, and 4) a skewed mean and median with potential data outliers removed. In all cases, a divider plate factor of 0.399 was used (i.e. an undegraded divider plate) to define the benefit of the divider plate in restricting tubesheet displacements.

Table 5: Limiting Crevice Pressure Ratios from 3 Models

	a,c,e
--	-------

From Section 1, the pressure ratio is defined as:

$$CP = S/P$$

Where CP is the crevice pressure ratio, P is the primary pressure and S is the secondary or measured tap pressure.

Therefore, the smallest pressure drop ($\Delta P = P - S$) occurs when the pressure ratio in Table 5 is the largest. The smallest pressure drop across the tube leads to the most conservative results since the contact pressure is minimized for tube retention and the driving head is maximized for leakage potential. The results from using the total data set, average or median, are provided for reference only, since each model predicts a non-conservative and physically unrealistic result.

Model 1 in Table 5, with the outliers excluded, yields the smallest pressure drop under SLB and the second smallest pressure drop under NOP conditions compared to Models 2 and 3 and also for the case where the outlier points are not excluded. Therefore, it is the worst case structural and leak resistance condition under SLB. It is also the second worst case structural and leak resistance condition under NOP. Model 1 also accurately captures the behavior of the crevice above the neutral axis of the tubesheet because the crevice pressure ratios for the NOP and SLB conditions are significantly different, as is expected. The table below summarizes the results of applying the three different models to the B* and H* analysis with a divider plate factor of 0.399.

Table 6: H* and B* Prediction for Different Models of Crevice Pressure
(Data based on improved tubesheet/divider plate structural model)

Model	Max. Contact Pressure		Max H* in	Max B* in
	SLB (psi)	NOP (Psi)		
[2.49	1.00
			6.11	1.00
			5.67	1.00
			5.15	1.00

a,c,e

(H* and B* are referenced to the bottom of the expansion transition)

The results prove that Model 1, using the skewed median values with the low outliers removed from the data set, is the most conservative approach to use when including the increased crevice pressure in the B* and H* analysis.

The following figures show the result of implementing the increased crevice pressure and divider plate restraint on the B* and H* analysis using Model 1. In order to compare the results using the new inputs to the results from the old inputs an existing B* and H* spreadsheet was used [10] and the necessary changes to the spreadsheet were checked and verified [11].

Figure 7 shows the original results for the B* and H* analysis for a typical model F steam generator cold leg assuming the secondary side pressure in the crevice and a divider plate factor of 0.76. The cold leg results are displayed in the plots below because they are typically limiting for a B* or H* analysis.

a,c,e



Figure 7: Unaltered Data and Methods for B* and H*. Crevice Pressure = $P_{Pri} - P_{Sec}$, DP = 0.76.

The results using the updated crevice pressure input with the updated divider plate factor of 0.399 are shown in Figure 8.

a,c,e



Figure 8: Updated Input Data and Methods for B* and H*. Crevice Pressure = $CP \cdot P_{Pri}$, DP = 0.399.

The results for the updated analysis input with a divider plate factor of 1.00 (i.e., no structural restraint provided by the divider plate) are shown in Figure 9.

a,c,e



Figure 9: Updated Input Data and Methods for B* and H*. Crevice Pressure = $CP \cdot P_{Pri}$, DP = 1.00.

Comparing the results shown in Figure 7 and Figure 9 proves that the changes in the B* and H* inputs due to the increased crevice pressure and divider plate effects are reasonable and follow similar trends compared to the prior results. The results shown in Figure 9 prove that the bounding analysis conditions in the event that the divider plate is fully degraded are still below the previously reported bounding value of 12.00 inches. The net effect on the final H* and B* values from increasing the crevice pressure is to increase the length of the tube required in the tubesheet to prevent tube pullout and maintain a factor of 2 on the SLB/NOP leak ratio when the updated divider plate factor is not included. This is a conservative result that is supported by test data. Therefore, the B* and H* criteria continue to be a valid approach to limiting the inspection distance of the tube portion within the tubesheet even when the revised conservative inputs for crevice pressure and divider plate function are included.

5.0 Summary and Conclusions

The following summarizes this "White Paper" regarding the effects of new test data and updated analysis methods on the H^*/B^* technical justifications:

1. Recently obtained test data indicate that postulated leakage through a tube crack in the tubesheet expansion region remains a single phase liquid and that the pressure decrease from the crack to essentially the top of the test specimens. The original H^*/B^* analysis assumed that the leakage through the crack flashes to steam immediately in the crevice, and that, therefore, the crevice pressure is at the secondary side pressure.
2. Updated finite element analysis of the tubesheet/divider plate assembly shows that the ratio of the maximum deflection of the tubesheet with an un-degraded divider plate to the maximum deflection with no structural restraint from the divider plate is much smaller than the factor derived from the original ASME Code Stress Report.
3. Analysis using the updated divider plate factor shows that the bounding value for H^*/B^* is about 12". Only the "true" B^* value will be affected if the divider plate is assumed to be non-functional. Significant margin exists for 17 inch inspection depth.
4. Several models were developed to represent the new crevice pressure test data. The most conservative model, that which minimizes the pressure drop from the primary side to the crevice, was identified.
5. Integrated analysis accounting for both the divider plate degradation and revised crevice pressure show that the justification for H^* and B^* is still valid when the most conservative crevice pressure model and the refined structural model for the tubesheet/divider plate assembly are used.

Enclosure III to WO 07-0012

**Westinghouse Electric Company LLC LTR CAW-07-2273, "Application for Withholding
Proprietary Information from Public Disclosure"**



Westinghouse Electric Company
Nuclear Services
P.O. Box 355
Pittsburgh, Pennsylvania 15230-0355
USA

U.S. Nuclear Regulatory Commission
Document Control Desk
Washington, DC 20555-0001

Direct tel: (412) 374-4419
Direct fax: (412) 374-4011
e-mail: maurerbf@westinghouse.com

Our ref: CAW-07-2273

April 24, 2007

APPLICATION FOR WITHHOLDING PROPRIETARY
INFORMATION FROM PUBLIC DISCLOSURE

Subject: LTR-CDME-07-72 P-Attachment, "Response to NRC Request for Additional Information Relating to LTR-CDME-05-209-P of the Wolf Creek Generating Station (WCGS) Permanent B* License Amendment Request," dated April 24, 2007 (Proprietary)

The proprietary information for which withholding is being requested in the above-referenced report is further identified in Affidavit CAW-07-2273 signed by the owner of the proprietary information, Westinghouse Electric Company LLC. The affidavit, which accompanies this letter, sets forth the basis on which the information may be withheld from public disclosure by the Commission and addresses with specificity the considerations listed in paragraph (b)(4) of 10 CFR Section 2.390 of the Commission's regulations.

Accordingly, this letter authorizes the utilization of the accompanying affidavit by Wolf Creek Nuclear Operating Corporation (WCNOC).

Correspondence with respect to the proprietary aspects of the application for withholding or the Westinghouse affidavit should reference this letter, CAW-07-2273, and should be addressed to J. A. Gresham, Manager, Regulatory Compliance and Plant Licensing, Westinghouse Electric Company LLC, P.O. Box 355, Pittsburgh, Pennsylvania 15230-0355.

Very truly yours,

A handwritten signature in black ink, appearing to read 'B. F. Maurer'.

B. F. Maurer, Acting Manager
Regulatory Compliance and Plant Licensing

Enclosures

cc: Jon Thompson (NRC O-7E1A)

bcc: J. A. Gresham (ECE 4-7A) 1L
R. Bastien, 1L (Nivelles, Belgium)
C. Brinkman, 1L (Westinghouse Electric Co., 12300 Twinbrook Parkway, Suite 330, Rockville, MD 20852)
RCPL Administrative Aide (ECE 4-7A) 1L (letter and affidavit only)
G. W. Whiteman, Waltz Mill
H. O. Lagally, Waltz Mill
C. D. Cassino, Waltz Mill
N. R. Brown, Waltz Mill
J. P. Molkenthin, Windsor

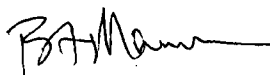
AFFIDAVIT

COMMONWEALTH OF PENNSYLVANIA:

ss

COUNTY OF ALLEGHENY:

Before me, the undersigned authority, personally appeared B. F. Maurer, who, being by me duly sworn according to law, deposes and says that he is authorized to execute this Affidavit on behalf of Westinghouse Electric Company LLC (Westinghouse), and that the averments of fact set forth in this Affidavit are true and correct to the best of his knowledge, information, and belief:



B. F. Maurer, Acting Manager
Regulatory Compliance and Plant Licensing

Sworn to and subscribed before me
this 24th day of April, 2007



Notary Public

COMMONWEALTH OF PENNSYLVANIA

Notarial Seal

Sharon L. Markle, Notary Public
Monroeville Boro, Allegheny County
My Commission Expires Jan. 29, 2011

Member, Pennsylvania Association of Notaries

- (1) I am Acting Manager, Regulatory Compliance and Plant Licensing, in Nuclear Services, Westinghouse Electric Company LLC (Westinghouse), and as such, I have been specifically delegated the function of reviewing the proprietary information sought to be withheld from public disclosure in connection with nuclear power plant licensing and rule making proceedings, and am authorized to apply for its withholding on behalf of Westinghouse.
- (2) I am making this Affidavit in conformance with the provisions of 10 CFR Section 2.390 of the Commission's regulations and in conjunction with the Westinghouse "Application for Withholding" accompanying this Affidavit.
- (3) I have personal knowledge of the criteria and procedures utilized by Westinghouse in designating information as a trade secret, privileged or as confidential commercial or financial information.
- (4) Pursuant to the provisions of paragraph (b)(4) of Section 2.390 of the Commission's regulations, the following is furnished for consideration by the Commission in determining whether the information sought to be withheld from public disclosure should be withheld.
 - (i) The information sought to be withheld from public disclosure is owned and has been held in confidence by Westinghouse.
 - (ii) The information is of a type customarily held in confidence by Westinghouse and not customarily disclosed to the public. Westinghouse has a rational basis for determining the types of information customarily held in confidence by it and, in that connection, utilizes a system to determine when and whether to hold certain types of information in confidence. The application of that system and the substance of that system constitutes Westinghouse policy and provides the rational basis required.

Under that system, information is held in confidence if it falls in one or more of several types, the release of which might result in the loss of an existing or potential competitive advantage, as follows:

- (a) The information reveals the distinguishing aspects of a process (or component, structure, tool, method, etc.) where prevention of its use by any of Westinghouse's competitors without license from Westinghouse constitutes a competitive economic advantage over other companies.

- (b) It consists of supporting data, including test data, relative to a process (or component, structure, tool, method, etc.), the application of which data secures a competitive economic advantage, e.g., by optimization or improved marketability.
- (c) Its use by a competitor would reduce his expenditure of resources or improve his competitive position in the design, manufacture, shipment, installation, assurance of quality, or licensing a similar product.
- (d) It reveals cost or price information, production capacities, budget levels, or commercial strategies of Westinghouse, its customers or suppliers.
- (e) It reveals aspects of past, present, or future Westinghouse or customer funded development plans and programs of potential commercial value to Westinghouse.
- (f) It contains patentable ideas, for which patent protection may be desirable.

There are sound policy reasons behind the Westinghouse system which include the following:

- (a) The use of such information by Westinghouse gives Westinghouse a competitive advantage over its competitors. It is, therefore, withheld from disclosure to protect the Westinghouse competitive position.
- (b) It is information that is marketable in many ways. The extent to which such information is available to competitors diminishes the Westinghouse ability to sell products and services involving the use of the information.
- (c) Use by our competitor would put Westinghouse at a competitive disadvantage by reducing his expenditure of resources at our expense.
- (d) Each component of proprietary information pertinent to a particular competitive advantage is potentially as valuable as the total competitive advantage. If competitors acquire components of proprietary information, any one component

may be the key to the entire puzzle, thereby depriving Westinghouse of a competitive advantage.

- (e) Unrestricted disclosure would jeopardize the position of prominence of Westinghouse in the world market, and thereby give a market advantage to the competition of those countries.
 - (f) The Westinghouse capacity to invest corporate assets in research and development depends upon the success in obtaining and maintaining a competitive advantage.
- (iii) The information is being transmitted to the Commission in confidence and, under the provisions of 10 CFR Section 2.390, it is to be received in confidence by the Commission.
- (iv) The information sought to be protected is not available in public sources or available information has not been previously employed in the same original manner or method to the best of our knowledge and belief.
- (v) The proprietary information sought to be withheld in this submittal is that which is appropriately marked in LTR-CDME-07-72 P-Attachment, "Response to NRC Request for Additional Information Relating to LTR-CDME-05-209-P of the Wolf Creek Generating Station (WCGS) Permanent B* License Amendment Request," dated April 24, 2007 (Proprietary), for submittal to the Commission, being transmitted by Wolf Creek Nuclear Operating Corporation (WCNOC) Application for Withholding Proprietary Information from Public Disclosure to the Document Control Desk. The proprietary information as submitted for use by Westinghouse for the Wolf Creek Generating Station is expected to be applicable to other licensee submittals in support of implementing a limited inspection of the tube joint within the tubesheet region of the steam generators and is provided in response to a NRC request for additional information on LTR-CDME-05-209-P, "Steam Generator Tube Alternate Repair Criteria for the Portion of the Tube Within the Tubesheet at Wolf Creek Generating Station," dated January 2006.

This information is part of that which will enable Westinghouse to:

- (a) Provide documentation of the analyses, methods, and testing for the implementation of an alternate repair criteria for the portion of the tubes within the tubesheet of the Wolf Creek Generating Station steam generators.
- (b) Assist the customer in obtaining NRC approval of the Technical Specification changes associated with the alternate repair criteria.

Further this information has substantial commercial value as follows:

- (a) Westinghouse plans to sell the use of similar information to its customers for the purposes of meeting NRC requirements for licensing documentation.
- (b) Westinghouse can sell support and defense of the technology to its customers in the licensing process.

Public disclosure of this proprietary information is likely to cause substantial harm to the competitive position of Westinghouse because it would enhance the ability of competitors to provide similar calculation, evaluation and licensing defense services for commercial power reactors without commensurate expenses. Also, public disclosure of the information would enable others to use the information to meet NRC requirements for licensing documentation without purchasing the right to use the information.

The development of the technology described in part by the information is the result of applying the results of many years of experience in an intensive Westinghouse effort and the expenditure of a considerable sum of money.

In order for competitors of Westinghouse to duplicate this information, similar technical programs would have to be performed and a significant manpower effort, having the requisite talent and experience, would have to be expended.

Further the deponent sayeth not.

PROPRIETARY INFORMATION NOTICE

Transmitted herewith are proprietary and/or non-proprietary versions of documents furnished to the NRC in connection with requests for generic and/or plant-specific review and approval.

In order to conform to the requirements of 10 CFR 2.390 of the Commission's regulations concerning the protection of proprietary information so submitted to the NRC, the information which is proprietary in the proprietary versions is contained within brackets, and where the proprietary information has been deleted in the non-proprietary versions, only the brackets remain (the information that was contained within the brackets in the proprietary versions having been deleted). The justification for claiming the information so designated as proprietary is indicated in both versions by means of lower case letters (a) through (f) located as a superscript immediately following the brackets enclosing each item of information being identified as proprietary or in the margin opposite such information. These lower case letters refer to the types of information Westinghouse customarily holds in confidence identified in Sections (4)(ii)(a) through (4)(ii)(f) of the affidavit accompanying this transmittal pursuant to 10 CFR 2.390(b)(1).

COPYRIGHT NOTICE

The reports transmitted herewith each bear a Westinghouse copyright notice. The NRC is permitted to make the number of copies of the information contained in these reports which are necessary for its internal use in connection with generic and plant-specific reviews and approvals as well as the issuance, denial, amendment, transfer, renewal, modification, suspension, revocation, or violation of a license, permit, order, or regulation subject to the requirements of 10 CFR 2.390 regarding restrictions on public disclosure to the extent such information has been identified as proprietary by Westinghouse, copyright protection notwithstanding. With respect to the non-proprietary versions of these reports, the NRC is permitted to make the number of copies beyond those necessary for its internal use which are necessary in order to have one copy available for public viewing in the appropriate docket files in the public document room in Washington, DC and in local public document rooms as may be required by NRC regulations if the number of copies submitted is insufficient for this purpose. Copies made by the NRC must include the copyright notice in all instances and the proprietary notice if the original was identified as proprietary.